Available online at www.sciencedirect.com
ScienceDirect
Ann. I. H. Poincaré – AN 26 (2009) 1237–1264
ANNALES DE L'INSTITUT HENRI POINCARÉ
ANALYSE NON LINÉAIRE
www.elsevier.com/locate/anihpc

Continuation of relative periodic orbits in a class of triatomic Hamiltonian systems

Guillaume James [a,*], Pascal Noble [b], Yannick Sire [c]

[a] *Institut National Polytechnique de Grenoble and CNRS, Laboratoire Jean Kuntzmann (UMR 5224), tour IRMA, BP 53, 38041 Grenoble Cedex 9, France*
[b] *Université de Lyon, Université Lyon 1, CNRS UMR 5208, Institut Camille Jordan, 43, boulevard du 11 novembre 1918, 69622 Villeurbanne Cedex, France*
[c] *Laboratoire d'Analyse Topologie Probabilités, UMR 6632, Université Aix-Marseille III, Faculté des Sciences et Techniques Saint-Jérôme, Avenue Escadrille Normandie-Niemen, 13397 Marseille Cedex 20, France*

Received 25 January 2008; received in revised form 12 October 2008; accepted 12 October 2008

Available online 30 October 2008

Abstract

We study relative periodic orbits (i.e. time-periodic orbits in a frame rotating at constant velocity) in a class of triatomic Euclidean-invariant (planar) Hamiltonian systems. The system consists of two identical heavy atoms and a light one, and the atomic mass ratio is treated as a continuation parameter. Under some nondegeneracy conditions, we show that a given family of relative periodic orbits existing at infinite mass ratio (and parametrized by phase, rotational degree of freedom and period) persists for sufficiently large mass ratio and for nearby angular velocities (this result is valid for small angular velocities). The proof is based on a method initially introduced by Sepulchre and MacKay [J.-A. Sepulchre, R.S. MacKay, Localized oscillations in conservative or dissipative networks of weakly coupled autonomous oscillators, Nonlinearity 10 (1997) 679–713] and further developed by Muñoz-Almaraz et al. [F.J. Muñoz-Almaraz, et al., Continuation of periodic orbits in conservative and Hamiltonian systems, Physica D 181 (2003) 1–38] for the continuation of normal periodic orbits in Hamiltonian systems. Our results provide several types of relative periodic orbits, which extend from small amplitude relative normal modes [J.-P. Ortega, Relative normal modes for nonlinear Hamiltonian systems, Proc. Roy. Soc. Edinburgh Sect. A 133 (2003) 665–704] up to large amplitude solutions which are not restrained to a small neighborhood of a stable relative equilibrium. In particular, we show the existence of large amplitude motions of *inversion*, where the light atom periodically crosses the segment between heavy atoms. This analysis is completed by numerical results on the stability and bifurcations of some inversion orbits as their angular velocity is varied.

Keywords: Continuation of relative periodic orbits; Euclidean-invariant Hamiltonian systems; Infinite mass ratio limit

1. Introduction

Hamiltonian systems of classical interacting particles are extensively used to study the vibrational dynamics of molecules or atomic clusters. In these models, nuclei interact via a strongly nonlinear potential that incorporates the

* Corresponding author.
E-mail addresses: guillaume.james@imag.fr (G. James), noble@math.univ-lyon1.fr (P. Noble), sire@cmi.univ-mrs.fr (Y. Sire).

0294-1449/$ – see front matter
doi:10.1016/j.anihpc.2008.10.002

effects of the electrons in the Born–Oppenheimer approximation. Despite this simplification, analyzing the dynamics of the resulting models remains a challenging problem.

In this context, a vast literature is focused on the existence and bifurcations of periodic orbits and their correspondence to the quantum mechanical eigenfunctions and quantum spectra (see e.g. [31,30,32] and their references). Such considerations can be extended to relative periodic orbits and equilibria, which are periodic or stationary in a frame rotating at constant velocity [33,14,13,25].

In this paper we consider a cluster B–A–B of three particles interacting in a plane, with two atoms B of identical masses and one lighter atom A (without loss of generality we fix to unity the mass of light atom A and denote by γ the mass of heavy atoms B). For simplicity we define the interaction energy via pair interaction potentials U, W (as done for example in reference [32]), but our results could be extended to more general Euclidean-invariant potentials. We focus on the existence of relative periodic orbits (this includes the particular case of periodic orbits) and restrict ourselves to rotations whose axis is perpendicular to the cluster plane. Our model is described by the Hamiltonian

$$\tilde{H} = \frac{1}{2\gamma}\big(\tilde{P}_1^2 + \tilde{P}_2^2\big) + \frac{1}{2}\tilde{p}_1^2 + U\big(\|\tilde{Q}_1 - \tilde{Q}_2\|\big) + W\big(\|\tilde{Q}_1 - \tilde{q}_1\|\big) + W\big(\|\tilde{Q}_2 - \tilde{q}_1\|\big), \tag{1}$$

where $\tilde{Q}_1, \tilde{Q}_2 \in \mathbb{R}^2$ (resp. $\tilde{q}_1$) are the positions of the heavy (resp. light) masses and $\tilde{P}_1, \tilde{P}_2, \tilde{p}_1$ their momenta. We assume that U, W are sufficiently smooth on $(0, +\infty)$ and the interaction forces U', W' vanish at some critical distances $D^*, d^* > 0$ with $U''(D^*) > 0$, $W''(d^*) > 0$ and $d^* > D^*/2$ (in order to allow triangular equilibrium configurations).

Classical approaches for proving the existence of periodic orbits in Hamiltonian systems rely on critical point theory [22] (see also [35,34] for applications to molecular potentials and more recent references), on the local Lyapunov center theorem [12] and Weinstein–Moser theorem [38,26], on global continuation techniques for Lyapunov families of periodic orbits (see [43] and its references) and degree theory for asymptotically linear Hamiltonian systems (see [8] and references therein).

In Hamiltonian systems with a continuous symmetry, the existence of relative periodic orbits around stable relative equilibria has been proved under general assumptions using extensions of the Weinstein–Moser theorem [15,28]. In addition, local continuation theorems for relative periodic orbits under small variations of energy and momentum are available [24,29,40] (see [25,39] and their references for the case of relative equilibria).

Here we examine relative periodic orbits using a continuation technique, which consists in varying the mass ratio between heavy and light atoms, starting from the infinite mass ratio limit. When the two atoms B have infinite mass, a class of solutions can be made by placing them in two static positions and letting the light atom A oscillate in the resulting potential. The distance between the two atoms B is obtained in turn as a critical point of an effective potential averaged over the orbit of mass A. We prove that relative periodic orbits of this system can be continued to finite mass ratio under some nondegeneracy conditions which are generally satisfied. A procedure of the same kind exists in the context of celestial mechanics as one passes from the restricted to the full three-body problem [1,23], with several important differences (some of which are outlined below). Moreover, the same idea has been used for studying time-periodic and spatially localized oscillations (discrete breathers) in one-dimensional diatomic Hamiltonian lattices [17].

One difficulty in our approach is due to the Euclidean invariance of the Hamiltonian system, which precludes a direct application of the implicit function theorem, replaced here by a technically involved Lyapunov–Schmidt reduction. As a benefit, the method provides large amplitude solutions which are not restrained to a small neighborhood of a relative equilibrium. Firstly, we obtain a family of relative periodic orbits on which internal oscillations extend from small amplitude normal modes up to large amplitude motions with arbitrarily large periods. Moreover, we show the existence of *inversions* where the light atom A crosses the B–B segment periodically. As their period is varied, these inversions form a one-parameter family of solutions which does not emerge from a relative equilibrium (they emerge from a pair of symmetric homoclinic orbits in the limit of infinite mass ratio). From a mathematical point of view, their existence in such systems was still an open problem up to our knowledge. Such solutions have been numerically computed in different models (see e.g. [32] and its references), but in system (1) their numerical continuation in energy was delicate [32]. Our continuation method, which starts from the simplified problem with infinite mass ratio, is numerically implemented in the present paper and provides an efficient way to compute these solutions.

It is interesting to compare our approach with related problems in celestial mechanics, which arise as one looks for relative periodic orbits of the full three-body problem by continuation from the restricted problem with one infinitesimal mass (see [1,23,7] and their references). Indeed, system (1) could be recast in a similar form (with a molecular

interaction potential replacing the gravitational one) after an appropriate time rescaling, and for small angular velocities. With this rescaled form of (1), two masses would be equal to 1 and one mass to $1/\gamma$. The static B–B stretch in the limit $\gamma \to +\infty$ would correspond in the context of celestial mechanics to a circular orbit of the Kepler problem viewed in a moving frame. However, a major simplification occurs in celestial mechanics since the interaction energy of the infinitesimal mass with each finite mass is small ($O(1/\gamma)$). As a consequence, in the restricted gravitational three-body problem the equations for the static B–B stretch and the light mass A are uncoupled, whereas they are coupled in the asymptotic limit of the triatomic system (1) since the potential W does not depend on γ. This coupling makes the analysis of periodic orbits more difficult.

As previously mentioned, the limit of infinite mass ratio was introduced by Livi, Spicci and MacKay [17] to prove the existence of discrete breathers in a one-dimensional Hamiltonian lattice known as the (diatomic) Fermi–Pasta–Ulam model. In this system, two types of atoms with different masses alternate on a one-dimensional lattice and interact anharmonically with their nearest neighbors. An uncoupled limit is obtained when the mass ratio between heavy and light atoms goes to infinity (light masses do not interact and oscillate in a local potential corresponding to immobile heavy masses). In this limit, the simplest type of discrete breather consists of a single particle oscillating while the others are at rest. As Livi et al. have shown, such localized solutions can be in general continued to large and finite mass ratio (see also [5] for numerical continuation results up to mass ratio equal to unity). The continuation procedure of reference [17] is simpler than the one in our triatomic system, because Euclidean invariance is trivially eliminated in the lattice by working with displacements between neighbors, whereas relative periodic orbits (periodic in a rotating frame) are analyzed in our case.

The approach of Livi et al. finds its roots in the former work of MacKay and Aubry [18] on the existence of breathers in one-dimensional chains of weakly coupled anharmonic oscillators. In the latter case, the uncoupled or "anti-continuum" limit is obtained by fixing the nearest-neighbors coupling constant to 0. The concept of anti-continuum limit characterized by large mass ratio has been subsequently applied to prove the existence of breathers in lattices of higher dimension invariant under translations [3]. In Ref. [19] a general strategy has been proposed for extending this result to (relative) discrete breathers in more general Hamiltonian systems invariant under rotations. A full existence proof was obtained by two of us in [10], but for reversible (even in time) and strictly time-periodic oscillations only. The approach presented in the present paper would allow to suppress such restrictions, since we obtain relative periodic orbits and nonreversible oscillations in triatomic systems using a method which would carry over to an arbitrary number of particles.

Now let us describe our continuation method in more detail. In Section 2 we reformulate the triatomic system using the classical Jacobi coordinates in order to eliminate the translational degeneracy. The equations are considered in a frame rotating at constant velocity, and time-periodic solutions (corresponding to relative periodic orbits) are searched in this rotating frame. We introduce a convenient scaling in order to analyze the resulting equations for large values of γ. The problem of finding periodic orbits is reformulated as a suitable functional equation in a loop space.

Section 3 is devoted to the limit case $\gamma = +\infty$. The limiting problem takes the form of a two degrees of freedom Hamiltonian system for the oscillations of light mass A coupled to a nonlinear integral constraint, both involving an unknown static B–B stretch. We restrict our attention to isosceles configurations, for which the Hamiltonian system becomes integrable with one degree of freedom. This allows us to obtain a global branch of periodic solutions for the system with nonlinear integral constraint (Theorem 1, p. 1251).

The continuation of relative periodic orbits to large and finite values of γ is performed in Section 4. Under some nondegeneracy conditions, we show that a given family of relative periodic orbits existing for $\gamma = +\infty$ (parametrized by phase, rotational degree of freedom and period) persists for large values of γ and nearby angular velocities (Theorem 2, p. 1255). Our analytical results are valid for small ($O(\gamma^{-1/2})$) angular velocities. In particular, Theorems 1 and 2 yield the existence of relative periodic orbits for the triatomic system with large mass ratio (Theorem 3, p. 1256). To complete these analytical results, we perform in Section 5 the numerical continuation of such solutions with respect to mass ratio and angular velocity, and study their stability properties.

The proof of Theorem 2 is based on the following method. To continue periodic solutions from $\gamma = +\infty$ to large values of γ we use a method introduced by Sepulchre and MacKay [37] for the continuation of normal periodic orbits in Hamiltonian systems (classical continuation results valid in less general situations can be found elsewhere, see e.g. [1], Chapter 8 or [23], Chapter 6 and their references). The theory developed by Sepulchre and MacKay has been generalized by Muñoz-Almaraz et al. [27] to treat more degenerate situations corresponding to Euclidean invariance. The first step is to introduce in the equations of motion artificial dissipative terms (with respect to energy,

angular momentum) multiplied by some damping coefficients α, β (this idea goes back to a work of Schmidt [36], who used this technique to derive the Lyapunov center theorem from Hopf's bifurcation theorem). The problem of finding periodic orbits is equivalent to searching for the zeros of a certain nonlinear operator, which is shown to be a *submersion* at a particular solution, thanks to the additional undetermined coefficients α, β. By the Lyapunov–Schmidt decomposition this yields a local family of periodic solutions (parametrized by their period, phase and rotational degree of freedom), which can be continued under small parameter changes. For time-periodic solutions, dissipative terms α, β are necessarily equal to 0, hence one recovers exact solutions of the original equations of motion. As show in this paper, this approach can be adapted to the present setting where $\gamma \to +\infty$ and relative periodic orbits are considered. This allows us to continue families of relative periodic orbits with respect to mass ratio and angular velocity.

2. Formulation of the problem

We consider the triatomic system previously introduced and described by the Hamiltonian (1). The linear momentum $P = \tilde{P}_1 + \tilde{P}_2 + \tilde{p}_1$ and the angular momentum $\tilde{J} = \tilde{Q}_1 \wedge \tilde{P}_1 + \tilde{Q}_2 \wedge \tilde{P}_2 + \tilde{q}_1 \wedge \tilde{p}_1$ are conserved quantities. We have introduced a tilde in the notations to indicate that we work in a fixed reference frame. The tilde will be suppressed when working in a rotating reference frame.

2.1. Choice of coordinates and scaling

Without loss of generality, we assume the center of mass of the triatomic system to be fixed at 0, i.e. $M(\tilde{Q}_1 + \tilde{Q}_2) + \tilde{q}_1 = 0$ (this is equivalent to working in a reference frame moving at constant velocity). This reduces the equations of motion (which correspond initially to a 12-dimensional differential equation) to a 8-dimensional system.

We shall use the notation $\gamma = \epsilon^{-2}$, the limit $\gamma \gg 1$ corresponding to $\epsilon \ll 1$. We search for oscillations which are time-periodic in a rotating reference frame with constant angular velocity $\Omega = \epsilon\bar{\omega}$, $\bar{\omega}$ being fixed and $\epsilon \approx 0$. We shall note Q_1, Q_2, q_1 the atomic positions in this new reference frame. The equations of motion for atomic positions can be rewritten as a Hamiltonian system in canonical form, with Hamiltonian

$$H = \frac{\epsilon^2}{2}\left(Y_1^2 + Y_2^2\right) + \frac{1}{2}y_1^2 - \Omega\left(Q_1^t K Y_1 + Q_2^t K Y_2 + q_1^t K y_1\right) + U\left(\|Q_1 - Q_2\|\right) + W\left(\|Q_1 - q_1\|\right) + W\left(\|Q_2 - q_1\|\right),$$

where Y_1, Y_2, y_1 are the variables conjugate to Q_1, Q_2, q_1 and $K = \left(\begin{smallmatrix} 0 & 1 \\ -1 & 0 \end{smallmatrix}\right)$. Note that $H = \tilde{H} - \Omega\tilde{J}$. Now we describe atomic positions using the Jacobi coordinates represented in Fig. 1 and defined by

$$u_1 = Q_2 - Q_1, \qquad u_2 = q_1 - \frac{1}{2}(Q_1 + Q_2). \tag{2}$$

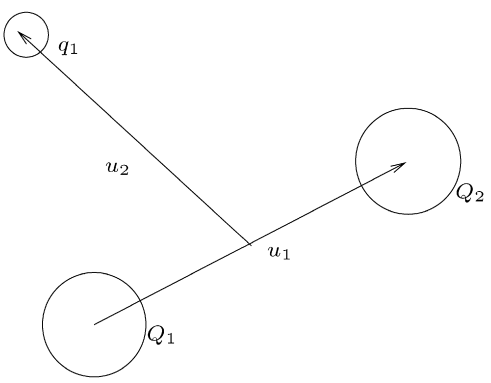

Fig. 1. Triatomic system and Jacobi coordinates.

The choice of Jacobi coordinates allows us to rewrite the triatomic system with fixed center of mass as a 8-dimensional Hamiltonian system in canonical form. The Hamiltonian reads

$$H = \epsilon^2\|w_1\|^2 + U\big(\|u_1\|\big) - \epsilon\bar{\omega}u_1^t K w_1 + \frac{1}{2}\left(1+\frac{\epsilon^2}{2}\right)\|w_2\|^2 + W\left(\left\|u_2+\frac{u_1}{2}\right\|\right) + W\left(\left\|u_2-\frac{u_1}{2}\right\|\right) - \epsilon\bar{\omega}u_2^t K w_2, \tag{3}$$

where w_1, w_2 are conjugate variables to u_1, u_2 and $w_1 = \frac{1}{2\epsilon^2}(\dot{u_1} - \epsilon\bar{\omega}Ku_1)$, $w_2 = (1+\frac{\epsilon^2}{2})^{-1}(\dot{u_2} - \epsilon\bar{\omega}Ku_2)$. Note that the degrees of freedom u_1, u_2 correspond to "reduced" masses $\epsilon^{-2}/2$ and $(1+\frac{\epsilon^2}{2})^{-1}$.

Now we look for time-periodic solutions (with fixed period T) as $\epsilon \to 0$ using an appropriate scaling. We set $u_1(t) = \bar{u} + \epsilon r_1(t)$ with

$$\int_0^T r_1(s)\,ds = 0, \tag{4}$$

and $w_1 = \epsilon^{-1}v_1$. In the sequel we shall rewrite for convenience $u_2 = r_2$, $w_2 = v_2$ and note $u^\perp = -Ku$. The equations of motion read

$$\begin{aligned} \dot{r}_1 &= 2v_1 - \bar{\omega}(\bar{u}+\epsilon r_1)^\perp, \qquad \dot{v}_1 = -\epsilon\big(\bar{\omega}v_1^\perp + \mathcal{F}_{\epsilon,\bar{u}}(r_1,r_2)\big),\\ \dot{r}_2 &= \left(1+\frac{\epsilon^2}{2}\right)v_2 - \epsilon\bar{\omega}r_2^\perp, \qquad \dot{v}_2 = -\epsilon\bar{\omega}v_2^\perp - \mathcal{G}_{\epsilon,\bar{u}}(r_1,r_2), \end{aligned} \tag{5}$$

where $\mathcal{F}_{\epsilon,\bar{u}}, \mathcal{G}_{\epsilon,\bar{u}} : \mathbb{R}^2 \times \mathbb{R}^2 \to \mathbb{R}^2$ are given by

$$\begin{aligned} \mathcal{F}_{\epsilon,\bar{u}}(r_1,r_2) &= U'\big(\|\bar{u}+\epsilon r_1\|\big)\frac{\bar{u}+\epsilon r_1}{\|\bar{u}+\epsilon r_1\|} + W'\left(\left\|r_2+\frac{\bar{u}+\epsilon r_1}{2}\right\|\right)\frac{r_2+\frac{\bar{u}+\epsilon r_1}{2}}{2\|r_2+\frac{\bar{u}+\epsilon r_1}{2}\|}\\ &\quad - W'\left(\left\|r_2-\frac{\bar{u}+\epsilon r_1}{2}\right\|\right)\frac{r_2-\frac{\bar{u}+\epsilon r_1}{2}}{2\|r_2-\frac{\bar{u}+\epsilon r_1}{2}\|},\\ \mathcal{G}_{\epsilon,\bar{u}}(r_1,r_2) &= W'\left(\left\|r_2+\frac{\bar{u}+\epsilon r_1}{2}\right\|\right)\frac{r_2+\frac{\bar{u}+\epsilon r_1}{2}}{\|r_2+\frac{\bar{u}+\epsilon r_1}{2}\|} + W'\left(\left\|r_2-\frac{\bar{u}+\epsilon r_1}{2}\right\|\right)\frac{r_2-\frac{\bar{u}+\epsilon r_1}{2}}{\|r_2-\frac{\bar{u}+\epsilon r_1}{2}\|}. \end{aligned} \tag{6}$$

The system (5) has two conserved quantities, namely the Hamiltonian

$$H = \|v_1\|^2 + U\big(\|\bar{u}+\epsilon r_1\|\big) - \bar{\omega}(\bar{u}+\epsilon r_1)^t K v_1 + \frac{1}{2}\left(1+\frac{\epsilon^2}{2}\right)\|v_2\|^2 + W\left(\left\|r_2+\frac{\bar{u}+\epsilon r_1}{2}\right\|\right) + W\left(\left\|r_2-\frac{\bar{u}+\epsilon r_1}{2}\right\|\right) - \epsilon\bar{\omega}r_2^t K v_2, \tag{7}$$

and the rescaled angular momentum $J = \epsilon\tilde{J}$ given by

$$J = \bar{u}\wedge v_1 + \epsilon(r_1\wedge v_1 + r_2\wedge v_2). \tag{8}$$

Moreover system (5) is reversible. Indeed, if $(\bar{u}, r_1, r_2)$ is a solution of the second-order system arising from (5) then $(-S\bar{u}, -Sr_1(-t), Sr_2(-t))$ is also a solution, where we denote by S the symmetry $S(a,b) = (-a,b)$.

The invariance of (5) under rotations will introduce technical difficulties for the continuation of periodic orbits since it excludes a direct application of the implicit function theorem. This invariance could be suppressed by using suitable internal coordinates (see e.g. [30,42,41,16] and their references). However these coordinates would introduce artificial singularities in the planar case [16], which would preclude the continuation of any singular periodic orbit.

2.2. Periodic orbits as zeros of a submersion

To analyze the limit $\epsilon \to 0$, we follow the approach initiated by MacKay and Sepulchre [37] for the continuation of periodic orbits in systems having a first integral and generalized by Muñoz-Almaraz et al. [27] to systems having several integrals. Let us sum up the strategy in a few lines. The starting point of the method is to introduce in the equations of motion artificial dissipative terms (with respect to energy, angular momentum) multiplied by some damping coefficients α, β. The problem of finding periodic orbits is equivalent to searching for the zeros of a certain nonlinear operator, which is shown to be a *submersion* at the points representing "normally degenerate" periodic solutions in the case $\epsilon = 0$, thanks to the additional undetermined coefficients α, β. We recall that a C^1 map $F : \mathbb{X} \to \mathbb{Y}$ between Banach spaces is a submersion at a point $X_0 \in \mathbb{X}$ if $DF(X_0)$ is surjective and its kernel has a closed complement in $\mathbb{X}$. By a Lyapunov–Schmidt decomposition we then find a local family of periodic solutions (parametrized by their period, phase and rotational degree of freedom), which can be continued to large values of γ and nearby angular velocities. For time-periodic solutions, it is proved that dissipative terms α, β are necessarily equal to 0, hence one recovers exact solutions of the original equations of motion.

To be more precise, we consider Eq. (5) with additional dissipative terms $\beta \nabla J$ and $\alpha \nabla H$. Rescaling time by $t \to t/T$, we work with 1-periodic functions of t and consider the period T as an unknown (for simplicity we shall keep the same notation r_i, v_i for the rescaled functions). Condition (4) becomes

$$\int_0^1 r_1(s)\,ds = 0. \tag{9}$$

One obtains the following differential system

$$\begin{aligned}
\dot r_1 &= T\big(2v_1 - \bar\omega(\bar u + \epsilon r_1)^\perp + \alpha\epsilon\big(\mathcal{F}_{\epsilon,\bar u}(r_1, r_2) + \bar\omega v_1^\perp\big) - \beta\epsilon v_1^\perp\big),\\
\dot v_1 &= T\big(-\epsilon\big(\bar\omega v_1^\perp + \mathcal{F}_{\epsilon,\bar u}(r_1, r_2)\big) + \alpha\big(2v_1 - \bar\omega(\bar u + \epsilon r_1)^\perp\big) + \beta(\bar u + \epsilon r_1)^\perp\big),\\
\dot r_2 &= T\left(\left(1 + \frac{\epsilon^2}{2}\right)v_2 - \epsilon\bar\omega r_2^\perp + \alpha\big(\epsilon\bar\omega v_2^\perp + \mathcal{G}_{\epsilon,\bar u}(r_1, r_2)\big) - \beta\epsilon v_2^\perp\right),\\
\dot v_2 &= T\left(-\epsilon\bar\omega v_2^\perp - \mathcal{G}_{\epsilon,\bar u}(r_1, r_2) + \alpha\left(\left(1 + \frac{\epsilon^2}{2}\right)v_2 - \epsilon\bar\omega r_2^\perp\right) + \beta\epsilon r_2^\perp\right).
\end{aligned} \tag{10}$$

In what follows we note $u = (r_1, r_2, v_1, v_2)^t$. The relation between the modified system (9), (10) and the original one (4), (5) is given by the following proposition.

Proposition 1. *Let u be a 1-periodic solution of* (9), (10) *and $\tilde u(t) = u(t/T)$. Assume there exists $t_0 \in \mathbb{R}$ such that $\nabla J(\tilde u(t_0))$ and $\nabla H(\tilde u(t_0))$ do not vanish and are not colinear. Then $\alpha = \beta = 0$ and $\tilde u$ is a T-periodic solution of* (4), (5).

Proof. Eq. (10) yields $\dot{\tilde u} = K\nabla H(\tilde u) + \alpha\nabla H(\tilde u) + \beta\nabla J(\tilde u)$ with $K = \left(\begin{smallmatrix} 0 & I \\ -I & 0 \end{smallmatrix}\right) \in M_8(\mathbb{R})$. We define $F(\tilde u) = \alpha H(\tilde u) + \beta J(\tilde u)$. Then $0 = \int_0^T \frac{d}{dt} F(\tilde u(t))\,dt = \int_0^T \|\nabla F(\tilde u(t))\|^2\,dt$ since H and J are first integrals of (5). Consequently $\nabla F(\tilde u(t)) = 0$ for all $t \in \mathbb{R}$, and $\alpha = \beta = 0$ follows by fixing $t = t_0$. □

Now we reformulate (10) as a suitable functional equation. As previously indicated, we shall derive a static equation satisfied by the degree of freedom $\bar u$ as $\epsilon = 0$. Since this static problem will inherit an invariance under rotation, we shall fix

$$\bar u = \bar\varrho(1, 0)^t \tag{11}$$

to eliminate this degeneracy. As a consequence we only need to determine a scalar equation satisfied by the static degree of freedom $\bar\varrho$. Multiplying by $\bar u$ the first two equations of (10), one obtains $\frac{1}{T}\int_0^1 (\dot v_1, \bar u)\,dt = \epsilon\mathcal{I}$, where $(\cdot,\cdot)$ denotes the canonical scalar product on $\mathbb{R}^2$ and

$$\mathcal{I} = -\big(1 + \alpha^2\big)\int_0^1 \big(\bar\omega v_1^\perp + \mathcal{F}_{\epsilon,\bar u}(r_1, r_2), \bar u\big)\,dt + \beta\int_0^1 \big(r_1^\perp + \alpha v_1^\perp, \bar u\big)\,dt. \tag{12}$$

In this computation we have used the fact that $\int_0^1 (\dot{r}_1, \bar{u})\,dt = 0$ due to time-periodicity. One has in the same way $\int_0^1 (\dot{v}_1, \bar{u})\,dt = 0$, hence $\mathcal{I} = 0$ for $\epsilon \neq 0$. For $\epsilon = 0$ we shall introduce the condition $\mathcal{I} = 0$ to fix the degree of freedom $\bar{u}$. The condition $\mathcal{I} = 0$ reads

$$\int_0^1 \big(\bar{\omega} v_1^{\perp} + \mathcal{F}_{\epsilon,\bar{u}}(r_1, r_2), \bar{u}\big)\,dt = \frac{\beta}{1+\alpha^2} \int_0^1 \big(r_1^{\perp} + \alpha v_1^{\perp}, \bar{u}\big)\,dt. \tag{13}$$

In the case $\alpha = \beta = 0$ that we shall recover at the end of our analysis (see Proposition 1), this condition becomes

$$\int_0^1 \big(\bar{\omega} v_1^{\perp} + \mathcal{F}_{\epsilon,\bar{u}}(r_1, r_2), \bar{u}\big)dt = 0. \tag{14}$$

Eqs. (10)–(13) can be rewritten as a functional equation

$$F_{\epsilon,\bar{\omega}}(r_1, v_1, r_2, v_2, \bar{\varrho}, T, \alpha, \beta) = 0 \tag{15}$$

with

$$F_{\epsilon,\bar{\omega}} = \begin{bmatrix} \dot{r}_1 - T(2v_1 - \bar{\omega}(\bar{u} + \epsilon r_1)^{\perp} + \alpha\epsilon(\mathcal{F}_{\epsilon,\bar{u}} + \bar{\omega} v_1^{\perp}) - \beta\epsilon v_1^{\perp}) \\ \dot{v}_1 - T(-\epsilon(\bar{\omega} v_1^{\perp} + \mathcal{F}_{\epsilon,\bar{u}}) + \alpha(2v_1 - \bar{\omega}(\bar{u} + \epsilon r_1)^{\perp}) + \beta(\bar{u} + \epsilon r_1)^{\perp} - \epsilon\mathcal{I}\frac{\bar{u}}{\|\bar{u}\|^2}) \\ \dot{r}_2 - T((1 + \frac{\epsilon^2}{2})v_2 - \epsilon\bar{\omega} r_2^{\perp} + \alpha(\epsilon\bar{\omega} v_2^{\perp} + \mathcal{G}_{\epsilon,\bar{u}}) - \beta\epsilon v_2^{\perp}) \\ \dot{v}_2 - T(-\epsilon\bar{\omega} v_2^{\perp} - \mathcal{G}_{\epsilon,\bar{u}} + \alpha((1 + \frac{\epsilon^2}{2})v_2 - \epsilon\bar{\omega} r_2^{\perp}) + \beta\epsilon r_2^{\perp}) \\ \mathcal{I} \end{bmatrix} \tag{16}$$

and $\bar{u} = \bar{\varrho}(1,0)^t$. Note that the second component of $F_{\epsilon,\bar{\omega}}$ multiplied by $(1,0)^t$ has 0 time-average (this is readily checked by multiplying this component by $\bar{u}$). For interaction potentials U, W sufficiently smooth on $(0, +\infty)$, the operator $F_{\epsilon,\bar{\omega}}$ is C^k from an open subset of the Hilbert space $\mathbb{X}$ into $\mathbb{Y}$, where $\mathbb{X} = \mathbb{H}^1_0 \times (\mathbb{H}^1)^3 \times \mathbb{R}^4$, $\mathbb{Y} = \mathbb{L}^2 \times \mathbb{L}^2_0 \times (\mathbb{L}^2)^2 \times \mathbb{R}$ and $\mathbb{H}^p$, $\mathbb{L}^2$ denote the classical Sobolev spaces $(H^p(\mathbb{T}))^2$, $(L^2(\mathbb{T}))^2$ ($\mathbb{T} = \mathbb{R}/\mathbb{Z}$). Moreover $r \in \mathbb{H}^1_0$ means $r \in \mathbb{H}^1$ and $\int_0^1 r(s)\,ds = 0$, and one notes $v \in \mathbb{L}^2_0$ if $v \in \mathbb{L}^2$ and $\int_0^1 (v(s), (1,0)^t)\,ds = 0$.

Particular solutions of the infinite mass ratio problem with $\epsilon = 0$ in (15) will be given in Section 3. More generally, we shall prove in Section 4 that $F_{0,\bar{\omega}_0}$ is a submersion at a given periodic solution of the infinite mass ratio problem with $\epsilon = 0$ and $\bar{\omega} = \bar{\omega}_0$, provided this solution fulfills certain nondegeneracy conditions. Then using the persistence of the zero set of a submersion under small perturbations, we shall obtain a family of periodic solutions of the full problem (10)–(13) when ϵ is small enough and $\bar{\omega} \approx \bar{\omega}_0$. By Proposition 1 this will yield a family of periodic solutions of (5).

3. Limit case of infinite mass ratio γ ($\epsilon = 0$)

3.1. Local families of periodic solutions

Let us consider the situation when $\epsilon = 0$ in (15) and study the existence of simple classes of small amplitude 1-periodic solutions. The differential system (10) reads

$$\begin{aligned} &\dot{r}_1 = T\big(2v_1 - \bar{\omega}\bar{u}^{\perp}\big), \qquad \dot{v}_1 = T\big(\alpha(2v_1 - \bar{\omega}\bar{u})^{\perp} + \beta\bar{u}^{\perp}\big), \\ &\dot{r}_2 = T\big(v_2 + \alpha\overline{\mathcal{G}}(\bar{u}, r_2)\big), \qquad \dot{v}_2 = T\big(-\overline{\mathcal{G}}(\bar{u}, r_2) + \alpha v_2\big), \end{aligned} \tag{17}$$

and the condition (13) can be written

$$\int_0^1 \big(\bar{\omega} v_1^{\perp} + \overline{\mathcal{F}}(\bar{u}, r_2), \bar{u}\big)\,dt = \frac{\beta}{1+\alpha^2} \int_0^1 \big(r_1^{\perp} + \alpha v_1^{\perp}, \bar{u}\big)\,dt, \tag{18}$$

with $\overline{\mathcal{F}}(\bar{u}, r_2) = \mathcal{F}_{0,\bar{u}}(0, r_2)$ and $\overline{\mathcal{G}}(\bar{u}, r_2) = \mathcal{G}_{0,\bar{u}}(0, r_2)$. We have $\overline{\mathcal{G}} = \nabla_{r_2} V$ and $\overline{\mathcal{F}} = \nabla_{\bar{u}} V$, the potential V being defined by $V(\bar{u}, r_2) = U(\|\bar{u}\|) + W(\|r_2 + \frac{\bar{u}}{2}\|) + W(\|r_2 - \frac{\bar{u}}{2}\|)$.

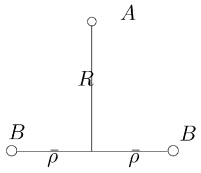

Fig. 2. Choice of coordinates for the triatomic system in an isosceles configuration.

Searching for 1-periodic solutions of (17), (18) satisfying the assumptions of Proposition 1, we obtain $\alpha = \beta = 0$ and thus

$$\begin{aligned}
&\dot r_1 = T(2v_1 - \bar\omega \bar u^\perp), \qquad \dot v_1 = 0,\\
&\dot r_2 = T v_2, \qquad \dot v_2 = -T\overline{\mathcal{G}}(\bar u, r_2),\\
&\int_0^1 \big(\bar\omega v_1^\perp + \overline{\mathcal{F}}(\bar u, r_2), \bar u\big)\, dt = 0.
\end{aligned} \tag{19}$$

Then we have $v_1 = \frac{1}{2}\bar\omega \bar u^\perp$ (since v_1 is constant and r_1 is time-periodic) and $r_1 = 0$ (since r_1 has 0 time-average). Recalling $\bar u = \bar\varrho(1,0)^t$ and after elimination of v_2 from the equations, problem (19) reduces to

$$\ddot r_2 + T^2 \nabla_{r_2} V\big(\bar\varrho(1,0)^t, r_2\big) = 0, \qquad \int_0^1 \overline{\mathcal{F}}_1\big(\bar\varrho(1,0)^t, r_2(s)\big)\, ds = \frac{\bar\omega^2}{2}\bar\varrho, \tag{20}$$

where $\overline{\mathcal{F}}_1$ is the first component of $\overline{\mathcal{F}}$. In the sequel we consider the case $\bar\omega = 0$ of (20) (the case $\bar\omega \approx 0$ will be later treated perturbatively, see Theorem 3).

For $\bar\omega = 0$, system (20) admits two symmetric triangular equilibrium solutions $(\bar u, r_2) = ((D^*, 0)^t, (0, \pm R^*)^t)$, where we note $R^* = (d^{*2} - \rho^{*2})^{1/2}$ and $\rho^* = D^*/2$. Other triangular equilibria are obtained by any rotation of these two equilibria. In addition there exist other equilibrium configurations where all atoms are aligned, with $r_2 = 0$ or $\bar u, r_2$ colinear.

Let us choose the triangular equilibrium $(\bar u^*, r_2^*) = ((D^*, 0)^t, (0, R^*)^t)$ and study some families of periodic solutions in its neighborhood. Since $W''(d^*) > 0$, the Hessian matrix $D^2_{r_2} V(\bar u^*, r_2^*)$ has two positive real eigenvalues $\omega_1^{*2} = 2W''(d^*)R^{*2}/d^{*2}$, $\omega_2^{*2} = W''(d^*)D^{*2}/(2d^{*2})$. As in the classical theory of Hamiltonian systems (the only difference here being the integral constraint of (20)) one can find a family of small amplitude nonlinear normal modes associated with each eigenvalue. This aspect is treated in detail in reference [10] for n-particle systems. Here we shall see how to obtain such solutions in a simple case.

In what follows we restrict our study to isosceles configurations with $\|Q_1 - q_1\| = \|Q_2 - q_1\|$ (see Fig. 2). Bifurcating solutions will be computed using the variables $r_2 = (0, R_2)$, $\bar\rho = \bar\varrho/2$ and we shall express the final results with the unscaled variable $R(t) = R_2(t/T)$. Problem (20) with $\bar\omega = 0$ becomes

$$R'' + \frac{\partial V_0}{\partial R}(R, \bar\rho) = 0, \tag{21}$$

$$\int_0^T \frac{\partial V_0}{\partial \bar\rho}\big(R(t), \bar\rho\big)\, dt = 0, \tag{22}$$

where R is $T-$periodic, $\bar\rho > 0$ and $V_0(R, \bar\rho) = 2W(\sqrt{R^2 + \bar\rho^2}) + U(2\bar\rho)$. System (21), (22) admits the equilibrium solutions $(R, \bar\rho) = (\pm R^*, \rho^*)$, i.e. $\nabla V_0(\pm R^*, \rho^*) = 0$.

In the isosceles configuration, the infinite mass ratio limit is considerably simpler to analyze because the differential equation (21) is integrable. However its phase space qualitatively depends on the variable $\bar\rho$ and Eq. (21) is coupled with the integral constraint (22). This will introduce technical difficulties in the global analysis of (21), (22) (Section 3.2). However, the local solution branch considered below can be easily computed using a classical treatment of pitchfork bifurcations.

In what follows we sketch the main arguments and refer to classical references [9,21,12] for more details on the analysis of pitchfork bifurcations. Setting $T = 2\pi/\Omega$, problem (21), (22) can be rewritten as a functional equation

$$G(R_2, \bar{\rho}, \Omega) = 0, \tag{23}$$

where $(R_2, \bar{\rho}) \in H^2_{ev}(\mathbb{R}/\mathbb{Z}) \times \mathbb{R}$ (the subscript ev in the notation of the Sobolev space refers to even functions of t),

$$G(R_2, \bar{\rho}, \Omega) = \left(\frac{\Omega^2}{4\pi^2} R_2'' + \frac{\partial V_0}{\partial R}(R_2, \bar{\rho}), \int_0^1 \frac{\partial V_0}{\partial \bar{\rho}}\big(R_2(t), \bar{\rho}\big)\, dt \right)$$

maps $H^2_{ev}(\mathbb{R}/\mathbb{Z}) \times (\mathbb{R}^+)^2$ into $L^2_{ev}(\mathbb{R}/\mathbb{Z}) \times \mathbb{R}$ and Ω plays the role of a bifurcation parameter. Now we examine the solutions of (23) near the trivial solution (R^*, ρ^*). Let us note that

$$D^2 V_0(R^*, \rho^*) = \begin{pmatrix} a & b \\ b & c \end{pmatrix}$$

where $a = \omega_1^{*2}$, $b = \omega_1^* \omega_2^*$ and $c = \omega_2^{*2} + 4U''(D^*)$. After elementary computations, one shows that $(R_2, \bar{\rho})$ belongs to the kernel of the operator $A_\Omega = D_{(R_2,\bar{\rho})} G(R^*, \rho^*, \Omega)$ if and only if

$$\frac{\Omega^2}{4\pi^2} R_2'' + a R_2 + b\bar{\rho} = 0, \quad \big(ac - b^2\big)\bar{\rho} = 0.$$

Since $D^2 V_0(R^*, \rho^*)$ is invertible (one has $U''(D^*) > 0$, $W''(d^*) > 0$) these conditions reduce to

$$R_2'' + 4\pi^2 \frac{\omega_1^{*2}}{\Omega^2} R_2 = 0, \quad \bar{\rho} = 0.$$

This linear problem has nontrivial solutions in $H^2_{ev}(\mathbb{R}/\mathbb{Z}) \times \mathbb{R}$ for $k\Omega = \omega_1^*$ ($k \in \mathbb{N}^*$), but it suffices to consider the case $k = 1$ (the other critical values of Ω yield in fact the same bifurcating solutions when one comes back to the unscaled problem (21)).

The kernel of $A_{\omega_1^*}$ is one-dimensional and spanned by $(R_2, \bar{\rho}) = (\cos 2\pi t, 0)$. Moreover problem (23) is invariant under the symmetry $R_2 \to R_2(t + 1/2)$, therefore a classical Lyapunov–Schmidt reduction [9,21,12] yields a bifurcation equation of pitchfork type

$$\alpha\big(\Omega - \omega_1^*\big) - \Omega_2 \alpha^3 + \mathrm{o}\big(|\alpha|\big|\Omega - \omega_1^*\big| + |\alpha|^3\big) = 0,$$

where α denotes the coordinate of bifurcating solutions along $\operatorname{Ker} A_{\omega_1^*}$. As a consequence, there exists a local branch of periodic solutions of (21)–(22) close to (R^*, ρ^*), which can be parametrized (up to phase shift) by

$$R(t) = R^* + \alpha \cos \Omega t + \mathrm{O}\big(\alpha^2\big), \tag{24}$$

$$\Omega = \omega_1^* + \mathrm{O}\big(\alpha^2\big), \tag{25}$$

$$\bar{\rho} = \rho^* + \mathrm{O}\big(\alpha^2\big), \tag{26}$$

where $\alpha \approx 0$ parametrizes the solution branch and $\Omega = 2\pi/T$ denotes the solution frequency. Note that $\bar{\rho}$ and Ω are even functions of α (changing α into $-\alpha$ is equivalent to shifting t by $T/2$), and we have fixed R even in t.

In addition there exists a second family of nonlinear normal modes, for which r_2 is even in time, admits two nontrivial components and the angle between $\bar{u}$ and r_2 oscillates around $\pi/2$. These modes correspond to the second eigenvalue ω_2^{*2}, and their existence can be proved by the same method as above, under the additional condition that ω_1^* is not a multiple of ω_2^* (for a slightly different method of proof see also [10], Theorem 1).

More generally, one can expect the existence of an infinity of families of periodic orbits (not necessarily time-reversible) arbitrarily close to the triangular equilibrium $(\bar{u}^*, r_2^*)$ as it is the case classically in two degree of freedom Hamiltonian systems, the only difference here being the integral constraint in (20). A way to obtain these solutions would be to select a family of periodic solutions r_2 (parametrized by $\bar{\rho}$ and its energy E) and study the zeros of the implicit function of $(\bar{\rho}, E)$ resulting from the integral constraint of (20) (see e.g. Fig. 6 in Section 3.2). This level set approach will be used in Section 3.2 to obtain global existence results for isosceles configurations. However, it could be used (at least locally) for more complex oscillations since $\overline{\mathcal{F}}_1(\bar{\varrho}(1,0)^t, r_2^*)$ changes its sign at $\bar{\varrho} = D^* = 2\rho^*$ (see Lemma 1), hence $\int_0^1 \overline{\mathcal{F}}_1(\bar{\varrho}(1,0)^t, r_2(s))\, ds$ will vanish at some value of $\bar{\varrho}$ if a periodic orbit r_2 is chosen sufficiently close to r_2^*.

3.2. Global solution branches

In this section we restrict ourselves to isosceles configurations where the atom A is equidistant from the two heavy atoms B. As we have seen previously, the problem reduces to an integrable differential equation for the position of A coupled with an integral constraint, both involving also the static B–B stretch. This simplified problem allows for a more detailed mathematical analysis including a global existence result. We make the following assumptions on the interaction potentials.

Hypothesis 1. The functions U, W are analytic over $\mathbb{R}^+$. Moreover, U', W' only vanish at some critical distance $D^*, d^* > 0$ respectively, with $U''(D^*) > 0$, $W''(d^*) > 0$ and $d^* > \rho^* = D^*/2$. In addition, W is a convex function on the interval $(0, d^*]$.

We recall that the assumption $d^* > \rho^*$ allows for triangular equilibrium configurations with $\|Q_i - q_1\| = d^*$, $\|Q_1 - Q_2\| = D^*$. The property of analyticity will be used to obtain global bifurcation results. The last convexity assumption could be relaxed but we prefer using it to simplify the analysis. This is not a severe restriction because the repulsive part of the potential turns out to be convex in many physical models.

Our analysis will provide two families of periodic solutions. The first one corresponds to the nonlinear normal modes (24)–(26) analytically continued in the large amplitude regime. The second solution family will be found to exist under appropriate conditions on W and U. It consists in *inversions* where the light atom A crosses the B–B segment. The two solution families are separated by an homoclinic orbit (corresponding to the limit of infinite period), where the atom A asymptotically approaches the B–B line center.

Note that the first solution branch could be obtained using general results from the analytic theory of global bifurcations [4], but we prefer to present a self-contained proof of global continuation which is based on elementary notions and yields more precise results. As previously mentioned, we shall reduce the analysis of (21), (22) to the study of a level line of an (implicitly defined) analytic function of two real variables.

3.2.1. A level set approach

It is first necessary to obtain suitable bounds for the solutions $\bar\rho$ of (21), (22), since the phase portrait of (21) qualitatively depends on $\bar\rho$.

Let us note that

$$\frac{1}{T}\int_0^T \frac{\partial V_0}{\partial \bar\rho}\big(R(t),\bar\rho\big)\,dt = 2U'(2\bar\rho) + 2\bar\rho\,\frac{1}{T}\int_0^T \frac{W'[(R(t)^2+\bar\rho^2)^{1/2}]}{(R(t)^2+\bar\rho^2)^{1/2}}\,dt,$$

which implies $\frac{1}{T}\int_0^T \frac{\partial V_0}{\partial \bar\rho}(R(t),\bar\rho)\,dt > 0$ when $\bar\rho \geqslant d^* > \rho^*$. As a consequence the solutions of (21), (22) necessarily satisfy $\bar\rho < d^*$.

With our assumptions on W, if $\bar\rho$ is fixed in the interval $(0, d^*)$ the potential $V_0(\cdot,\bar\rho)$ has a double well structure, with three critical points $R = 0$ and $R = \pm R_0(\bar\rho)$, with $R_0(\bar\rho) = (d^{*2} - \bar\rho^2)^{1/2}$ (see Fig. 3). The equilibria $R = \pm R_0(\bar\rho)$ of (21) are elliptic and $R = 0$ is a saddle point. The hardness coefficient

$$h(\bar\rho) = \left[\frac{\partial^2 V_0}{\partial R^2}\frac{\partial^4 V_0}{\partial R^4} - \frac{5}{3}\left(\frac{\partial^3 V_0}{\partial R^3}\right)^2\right]_{R=R_0(\bar\rho)} \tag{27}$$

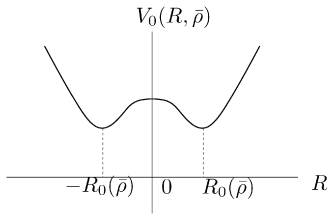

Fig. 3. Local shape of the potential $V_0(\cdot,\bar\rho)$ having a double well structure for $\bar\rho \in (0, d^*)$. In the case represented here, $V_0(\cdot,\bar\rho)$ has a local maximum at $R = 0$ and a global one at infinity. This case occurs for $\bar\rho$ sufficiently close to d^*.

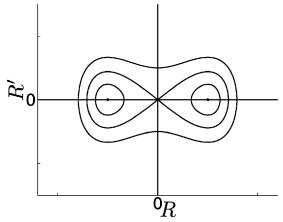

Fig. 4. Phase space of Eq. (21) for $\bar\rho \in (d_{\min}, d^*)$, in the vicinity of the two symmetric homoclinic orbits.

determines (depending on whether $h > 0$ or $h < 0$) if the frequency of oscillations around $R_0(\bar\rho)$ locally increases or decreases with amplitude (we shall use this property in Appendix A).

Since W is strictly increasing (respectively decreasing) on the interval $(d^*, +\infty)$ (respectively on $(0, d^*)$) we define

$$d_{\min} = \mathrm{Inf}\big\{d \in (0, d^*),\, W(d) < W_\infty\big\},$$

where we note $W_\infty = \lim_{x\to+\infty} W(x)$ (W_∞ is either finite or equal to $+\infty$). If $\bar\rho$ lies within the interval $(d_{\min}, d^*)$, one has $W(\bar\rho) < W_\infty$ and thus $V_0(0, \bar\rho) < \lim_{R\to+\infty} V_0(R, \bar\rho)$. This means $V_0(\cdot, \bar\rho)$ has a local maximum at $R = 0$ and a global one at infinity. In that case, the trajectories of (21) have the structure shown in Fig. 4 at least locally, with a pair of symmetric homoclinic orbits to $R = 0$. The periodic orbits inside the homoclinic loops correspond to nonlinear normal modes, and the periodic orbits lying outside correspond to inversions of the atom A. The set of periodic orbits outside the homoclinic loops qualitatively depends on the behavior of W at infinity. If $W_\infty = +\infty$, the surrounding periodic orbits represented in Fig. 4 fill the entire phase space around the homoclinic loops. If $W_\infty < +\infty$, they are confined in a region bounded by a pair of symmetric heteroclinic orbits (joining $(R, R') = (\pm\infty, 0)$), and no periodic orbits exists outside.

In the sequel we assume $\rho^* > d_{\min}$. Consequently, one has $\bar\rho \in (d_{\min}, d^*)$ when $\alpha \approx 0$ is slightly increased along the local solution branch (24)–(26) (in fact we shall see later that $\rho^* \leqslant \bar\rho$ on this solution branch). Therefore, (R, R') corresponds in Fig. 4 to the trajectory of period T close to the elliptic equilibrium $(R_0(\bar\rho), 0)$.

Remark 1. The case $\rho^* < d_{\min}$ will not be considered here but could be treated with similar methods. In that case the solution branch would have different properties, because homoclinic bifurcations occur in Eq. (21) as $\bar\rho$ exits the interval $(d_{\min}, d^*)$ due to qualitative changes in the potential V_0. If $d_{\min} > 0$ (which implies W and V_0 have a finite limit at $+\infty$) and $\bar\rho = d_{\min}$, then V_0 admits three global maxima at $R = -\infty, 0, +\infty$. For $\bar\rho \in (0, d_{\min})$, there is one global maximum at $R = 0$ and two "local" maxima at $R = \pm\infty$.

Now we develop a simple level set approach to obtain global branches of periodic solutions. For this purpose, we parametrize the periodic orbits by their energy difference E with respect to the ground state energy. More precisely we have

$$E = 2\big[W\big(\sqrt{R(0)^2 + \bar\rho^2}\big) - W(d^*)\big]$$

(we have fixed R even in t). The value $E = 0$ corresponds to the equilibrium solution $R = R_0(\bar\rho)$, and R approaches an homoclinic orbit to 0 as $E \to E_{\max}(\bar\rho)$ defined by $E_{\max}(\bar\rho) = 2(W(\bar\rho) - W(d^*))$ ($E_{\max}(\bar\rho)$ is the energy difference between the unstable equilibrium $R = 0$ and the ground state $R_0(\bar\rho)$). As we move along the family of periodic orbits outside the homoclinic orbit, E increases from $E_{\max}(\bar\rho)$ to the maximal value $E^* = 2(W_\infty - W(d^*))$. One has $E^* = +\infty$ (and $d_{\min} = 0$) when W is unbounded at $+\infty$. If W is bounded at $+\infty$, the limiting value $E^* < \infty$ corresponds to a pair of symmetric heteroclinic orbits joining $(R, R') = (\pm\infty, 0)$.

To each value $E \in [0, E_{\max}(\bar\rho)) \cup (E_{\max}(\bar\rho), E^*)$ corresponds a unique solution $R_{E,\bar\rho}$ of (21) with $R'(0) = 0$ and $R(0) \geqslant R_0(\bar\rho)$. We shall note $T_{E,\bar\rho}$ its period. Due to the analyticity of W (which implies in particular the analyticity of $R(t)$ with respect to initial conditions), and since $W'(d)$ vanishes only at $d = d^*$ (yielding $\frac{\partial E}{\partial R(0)} > 0$ for $R(0) > R_0(\bar\rho)$), the solution $R_{E,\bar\rho}$ depends analytically on $(t, E, \bar\rho)$ for $t \in \mathbb{R}$ and $(E, \bar\rho)$ in the open domain $\Lambda = \Lambda_i \cup \Lambda_o$ with

$$\Lambda_i = \big\{(E, \bar\rho) \in \mathbb{R}^+ \times (d_{\min}, d^*),\, 0 < E < E_{\max}(\bar\rho)\big\}, \tag{28}$$

$$\Lambda_o = \big\{(E, \bar\rho) \in \mathbb{R}^+ \times (d_{\min}, d^*),\, E_{\max}(\bar\rho) < E < E^*\big\}. \tag{29}$$

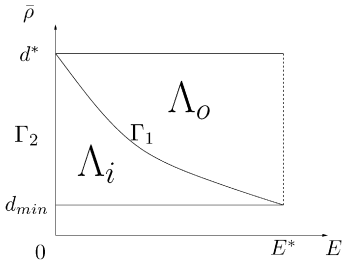

Fig. 5. Open domain $\Lambda = \Lambda_i \cup \Lambda_o$ defined by (28), (29) and parts Γ_1, Γ_2 of its boundary defined by (30), (31).

The domain Λ is depicted in Fig. 5. In the sequel we note Γ_1, Γ_2 the parts of $\partial\Lambda$ defined by

$$\Gamma_1 = \big\{(E,\bar{\rho}),\, E = E_{\max}(\bar{\rho}),\, \bar{\rho} \in (d_{\min}, d^*)\big\}, \tag{30}$$

$$\Gamma_2 = \big\{(E,\bar{\rho}),\, E = 0,\, \bar{\rho} \in (d_{\min}, d^*)\big\}. \tag{31}$$

To solve Eq. (22) we now introduce

$$f(E,\bar{\rho}) = \frac{1}{T_{E,\bar{\rho}}} \int_0^{T_{E,\bar{\rho}}} \frac{\partial V_0}{\partial \bar{\rho}}\big(R_{E,\bar{\rho}}(t),\bar{\rho}\big)\,dt. \tag{32}$$

Solving system (21), (22) is equivalent to computing the level set $f = 0$, and each point $(E,\bar{\rho})$ on this level set corresponds to a unique solution $(R,\bar{\rho}) = (R_{E,\bar{\rho}},\bar{\rho})$. The function f is analytic on Λ (due to the analyticity of $R_{E,\bar{\rho}}$ and $T_{E,\bar{\rho}}$), and can be extended to a continuous function on the domain

$$\bar{\Lambda} = \Lambda \cup \Gamma_1 \cup \Gamma_2 \tag{33}$$

(note that $\bar{\Lambda}$ is different here from the closure of Λ). Clearly $f(0,\bar{\rho}) = \frac{\partial V_0}{\partial \bar{\rho}}(R_0(\bar{\rho}),\bar{\rho})$ and consequently

$$f(0,\bar{\rho}) = 2U'(2\bar{\rho}). \tag{34}$$

Moreover, since $R_{E,\bar{\rho}}$ approaches an homoclinic orbit to 0 as $E \to E_{\max}(\bar{\rho})^-$ (and a pair of symmetric homoclinics as $E \to E_{\max}(\bar{\rho})^+$) one has consequently $\lim_{E\to E_{\max}(\bar{\rho})} T_{E,\bar{\rho}} = +\infty$ and

$$\lim_{E\to E_{\max}(\bar{\rho})} \frac{1}{T_{E,\bar{\rho}}} \int_0^{T_{E,\bar{\rho}}} \frac{\partial V_0}{\partial \bar{\rho}}\big(R_{E,\bar{\rho}}(t),\bar{\rho}\big)\,dt = \frac{\partial V_0}{\partial \bar{\rho}}(0,\bar{\rho}).$$

It follows

$$f\big(E_{\max}(\bar{\rho}),\bar{\rho}\big) = 2\big(W'(\bar{\rho}) + U'(2\bar{\rho})\big). \tag{35}$$

Similarly to (33) we shall note in the sequel $\bar{\Lambda}_i = \Lambda_i \cup \Gamma_1 \cup \Gamma_2$, $\bar{\Lambda}_o = \Lambda_o \cup \Gamma_1 \cup \Gamma_2$. The following technical lemma will be useful to analyze the level set $f = 0$.

Lemma 1. *Assume Hypothesis* 1 *is satisfied and* $d_{\min} < \rho^*$. *Then the function* f *defined on* $\bar{\Lambda}$ *possesses the following properties for* $(E,\bar{\rho}) \in \bar{\Lambda}_i$:

(i) $f(0,\bar{\rho}) < 0$ *if* $\bar{\rho} < \rho^*$ *and* $f(0,\bar{\rho}) > 0$ *if* $\bar{\rho} > \rho^*$.
(ii) $f(E,\bar{\rho}) < f(0,\bar{\rho})$ *if* $E > 0$.
(iii) $f(E,\bar{\rho}) < 0$ *if* $0 < E \leqslant E_{\max}(\bar{\rho})$ *and* $\bar{\rho} \leqslant \rho^*$.
(iv) *There exists an interval* $[\bar{\rho}_1, d^*]$ *(with* $\bar{\rho}_1 > \rho^*$*) on which* $f(E_{\max}(\bar{\rho}),\bar{\rho})$ *is strictly positive.*
(v) $f(E,\bar{\rho}) > f(E_{\max}(\bar{\rho}),\bar{\rho})$ *if* $0 \leqslant E < E_{\max}(\bar{\rho})$.
(vi) *There exists* $m > 0$ *such that* $f(E,\bar{\rho}) \geqslant m$ *for* $\bar{\rho}_1 \leqslant \bar{\rho} < d^*$ *and* $0 \leqslant E \leqslant E_{\max}(\bar{\rho})$.

Proof. Property (i) simply follows from equality (34).

Let us prove properties (ii) and (iii). We have by definition

$$f(E,\bar{\rho}) = 2\left(U'(2\bar{\rho}) + \frac{\bar{\rho}}{T_{E,\bar{\rho}}}\int_0^{T_{E,\bar{\rho}}} \frac{W'[(R_{E,\bar{\rho}}(t)^2+\bar{\rho}^2)^{1/2}]}{(R_{E,\bar{\rho}}(t)^2+\bar{\rho}^2)^{1/2}}\,dt\right). \tag{36}$$

Since $R_{E,\bar{\rho}}$ satisfies

$$R''_{E,\bar{\rho}} + 2R_{E,\bar{\rho}}\frac{W'[({R_{E,\bar{\rho}}}^2+\bar{\rho}^2)^{1/2}]}{({R_{E,\bar{\rho}}}^2+\bar{\rho}^2)^{1/2}} = 0, \tag{37}$$

and $R_{E,\bar{\rho}}(t)$ does not vanish, one obtains by substituting (37) into (36) and integrating by parts

$$f(E,\bar{\rho}) = 2U'(2\bar{\rho}) - \frac{\bar{\rho}}{T_{E,\bar{\rho}}}\int_0^{T_{E,\bar{\rho}}}\left(\frac{R'_{E,\bar{\rho}}}{R_{E,\bar{\rho}}}\right)^2 dt. \tag{38}$$

Using (34) it follows $f(E,\bar{\rho}) < f(0,\bar{\rho})$, since the last term in the sum is strictly negative for $E>0$. This proves (ii), and property (iii) follows by combining properties (ii) and (i).

Property (iv) follows directly from equality (35). Let us now prove property (v). The case $E=0$ is straightforward and there remains to examine the case $0<E<E_{\max}(\bar{\rho})$. Using (38) we find

$$f(E,\bar{\rho}) > 2U'(2\bar{\rho}) - \bar{\rho}\left\|\frac{R'_{E,\bar{\rho}}}{R_{E,\bar{\rho}}}\right\|^2_{L^\infty(0,T_{E,\bar{\rho}})}. \tag{39}$$

Now we use the fact that Eq. (21) is integrable, with trajectories given by $R'^2 = g_E((R^2+\bar{\rho}^2)^{1/2})$ and $g_E(d) = 2[E + 2W(d^*) - 2W(d)]$. On each periodic orbit, $d = (R^2+\bar{\rho}^2)^{1/2}$ belongs to some interval $[d_-(E), d_+(E)]$ increasing with E, with $d_-(E)\to\bar{\rho}^+$ as $E\to E_{\max}(\bar{\rho})^-$. In addition, the maximal value of g_E/R^2 is necessarily attained on the interval $[d_-(E), d^*]$ where g_E is increasing. Consequently we have the estimate

$$f(E,\bar{\rho}) > 2U'(2\bar{\rho}) - \bar{\rho}\left\|\frac{g_E}{d^2-\bar{\rho}^2}\right\|_{L^\infty(d_-(E),d^*)}. \tag{40}$$

Since g_E increases with E, one obtains the estimate

$$f(E,\bar{\rho}) > 2U'(2\bar{\rho}) - \bar{\rho}\left\|\frac{g}{d^2-\bar{\rho}^2}\right\|_{L^\infty(\bar{\rho},d^*)}, \tag{41}$$

where $g = g_{E_{\max}(\bar{\rho})}$ is given by $g(d) = 4[W(\bar{\rho}) - W(d)]$. More intuitively, this estimate comes from the fact that the slope at the origin (R'/R) is maximal on the surrounding homoclinic orbit (see Fig. 4). Now the concavity of g on the interval $(0, d^*]$ yields

$$\left\|\frac{g-g(\bar{\rho})}{d^2-\bar{\rho}^2}\right\|_{L^\infty(\bar{\rho},d^*)} = \frac{g'(\bar{\rho})}{2\bar{\rho}}$$

hence $f(E,\bar{\rho}) > 2\big(U'(2\bar{\rho}) + W'(\bar{\rho})\big)$, which proves (v). Property (vi) follows directly from (iv) and (v). □

3.2.2. Global solution branches

We are now ready to study the level line

$$\Delta_0 = \big\{(E,\bar{\rho})\in\bar{\Lambda},\, f(E,\bar{\rho}) = 0\big\}.$$

For this purpose we consider the local solution branch defined by (24)–(26). In a neighborhood of $(E,\bar{\rho}) = (0,\rho^*)$, it provides a (locally unique) smooth curve on which f vanishes. This curve can be parametrized by $E\approx 0$ and we have $\bar{\rho} = \rho^* + \mathrm{O}(E)$.

Due to the analyticity of f in Λ_i, the curve cannot end at one point in Λ_i. Moreover, using Lemma 1, $\Delta_0\cap\bar{\Lambda}_i$ lies necessarily in the strip $\rho^*\leqslant\bar{\rho}<\bar{\rho}_1$ (see properties (i), (iii) and (vi)) and intersects the boundary Γ_2 only at

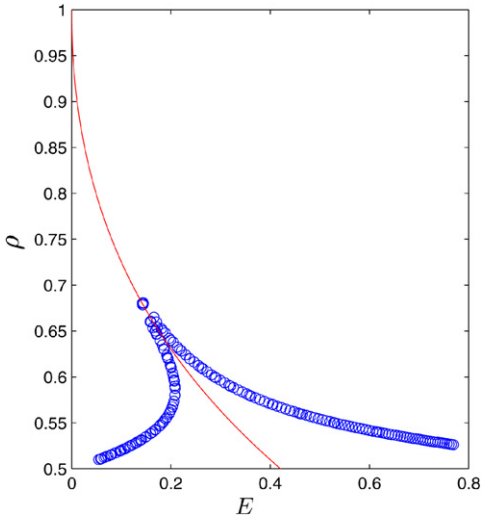

Fig. 6. Level line Δ_0 (thick line) computed numerically for the Morse potentials $U(x) = W(x) = \frac{1}{2}(e^{-(x-1)} - 1)^2$. The thin line represents Γ_1. The thick line extends in fact up to $(E_0, \rho_0) \approx (0.04, 0.81) \in \Gamma_1$, but the two lines become indistinguishable closer to this point at the figure resolution. This computation suggests that Δ_0 and Γ_1 are tangent at (E_0, ρ_0) where Δ_0 forms a cusp.

$(E, \bar{\rho}) = (0, \rho^*)$ (see property (i)). Consequently, there exists a connected subset of Δ_0 joining $(E, \bar{\rho}) = (0, \rho^*)$ to a point $(E_0, \rho_0) \in \Gamma_1$ (which might not be unique) with $\rho^* < \rho_0 < \bar{\rho}_1$. In the sequel we note $\tilde{\Delta}_0$ the maximal connected component of Δ_0 containing $(E, \bar{\rho}) = (0, \rho^*)$ and (E_0, ρ_0).

The zeros of $f(E_{\max}(\bar{\rho}), \bar{\rho})$ (defined by Eq. (35)) determine the intersection points between Δ_0 and Γ_1 (there is at least one intersection point and only a finite number). It is worthwhile to note that these intersection points have a simple interpretation with respect to the Hamiltonian (1). If $f(E_{\max}(\bar{\rho}), \bar{\rho}) = 0$, there exists an equilibrium of (1) where the light atom A lies in the middle of the B–B bond (i.e. $R = 0$) at a distance $\bar{\rho}$ from the two heavy atoms B (expression (35) gives the force exerted on one atom B by the two remaining atoms A, B in this configuration).

Without loss of generality, we now assume the existence of a path in $\tilde{\Delta}_0$ which connects $(0, \rho^*)$ to (E_0, ρ_0) without intersecting Γ_1 at an other point. To simplify the discussion we assume that $\bar{\rho} = \rho_0$ is a simple zero of $f(E_{\max}(\bar{\rho}), \bar{\rho})$. Consequently $f(E_{\max}(\bar{\rho}), \bar{\rho})$ changes its sign at $\bar{\rho} = \rho_0$, and the curve $\tilde{\Delta}_0$ can be continued across Γ_1 inside the domain Λ_o.

As one approaches the point (E_0, ρ_0) on $\tilde{\Delta}_0$, or any other point in $\Delta_0 \cap \Gamma_1$, the period $T_{E,\bar{\rho}}$ of the corresponding solution of (21) tends to infinity. For $(E, \bar{\rho}) \in \Lambda_i$ the corresponding solutions of (21) consist in periodic orbits inside an homoclinic orbit to 0 (see Fig. 4). For $(E, \bar{\rho}) \in \Lambda_o$ they consist in periodic orbits lying outside.

Since a curve of solutions of $f = 0$ emanating from (E_0, ρ_0) cannot end at one point in Λ_o, this curve is either unbounded (this is possible only if $E^* = +\infty$, i.e. for W unbounded at infinity) or reaches again the boundary of Λ_o. It cannot reach the line $d = d^*$ as we noted previously.

To illustrate these results, let us consider the case when U and W are equal and defined as a Morse potential

$$U(x) = W(x) = \frac{1}{2}\big(e^{-(x-1)} - 1\big)^2.$$

One has $d^* = D^* = 1$ (hence $\rho^* = 1/2$) and one finds $d_{\min} = 1 - \ln 2 < \rho^*$. Moreover the function f vanishes on Γ_1 at a unique point $(E_0, \rho_0) \approx (0.04, 0.81)$. The level line Δ_0 can be numerically computed and is shown in Fig. 6.

It is also worthful to note that solutions of (21), (22) satisfy $\bar{\rho} > d_{\min}$ if $\rho^* > d_{\min}$. Indeed, for $\bar{\rho} \leqslant d_{\min}$, $R(t)$ does not vanish on any periodic orbit (this is in connection with Remark 1) and we find $\int_0^T \frac{\partial V_0}{\partial \bar{\rho}}(R(t), \bar{\rho})\, dt < 0$ using formula (38). Consequently we have necessarily $d_{\min} < \bar{\rho} < d^*$, i.e. all solutions $\bar{\rho}$ lie in our domain of study.

Our analysis of the level set $f(E, \bar{\rho}) = 0$ provides global branches of solutions of system (21), (22). These solutions are $(R, \bar{\rho}) = (R_{E,\bar{\rho}}, \bar{\rho})$ where $(E, \bar{\rho})$ is any point on the level line, except the points on Γ_1 (which would correspond to an infinite period). These results are summarized in Theorem 1, which provides a global branch of nonlinear normal modes (see property (i) below) and a family of solutions with arbitrarily large periods corresponding to inversions of the light atom A (property (ii)).

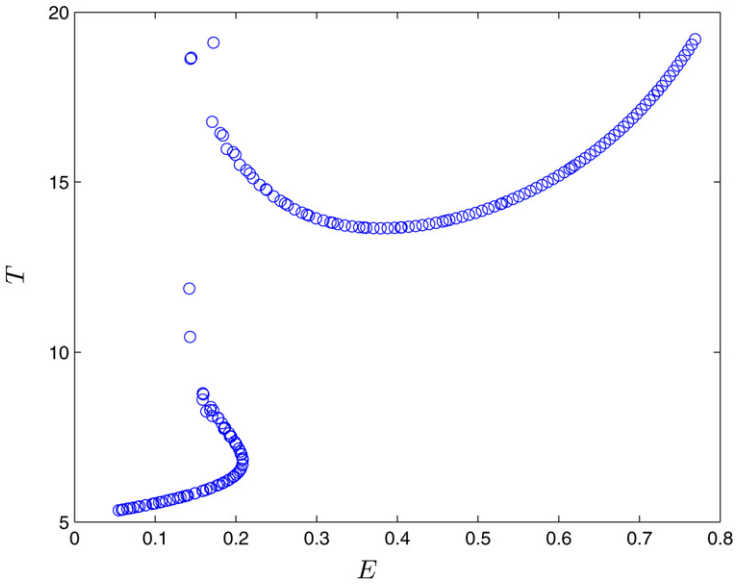

Fig. 7. Period of the orbit of (21) with energy difference E as $(E, \bar{\rho})$ are varied along the level line $f(E, \bar{\rho}) = 0$, for $U(x) = W(x) = \frac{1}{2}(e^{-(x-1)} - 1)^2$.

We note $C_b^2(\mathbb{R})$ the space of C^2 bounded functions over $\mathbb{R}$ with bounded derivatives, and R_ρ^h the positive solution of (21) homoclinic to 0 (fixed even it t) which exists for $\bar{\rho} \in (d_{\min}, d^*)$. The zero $\bar{\rho} = \rho_0$ of the function $f(E_{\max}(\bar{\rho}), \bar{\rho})$ referred to in Theorem 1 has been defined at the beginning of Section 3.2.2.

Theorem 1. *Assume Hypothesis* 1 *is satisfied,* $d_{\min} < \rho^*$ *and the zero* $\bar{\rho} = \rho_0$ *of* $f(E_{\max}(\bar{\rho}), \bar{\rho})$ *is simple. Then the following properties hold.*

(i) *For all* $\bar{\rho} \in (\rho^*, \rho_0)$*, there exists* $T > 0$ *and a* T*-periodic function* R *satisfying* (21), (22)*,* $0 < E < E_{\max}(\bar{\rho})$ *and the following properties*:
  (a) R *is even in* t*,* $R(t) > 0$ *for all* $t \in \mathbb{R}$*,*
  (b) $T \to 2\pi/\omega_1^*$*,* $E \to 0$ *and* $R \to R^*$ *in* $C_b^2(\mathbb{R})$ *as* $\bar{\rho} \to \rho^*$*. In this limit the solutions can be parametrized by* (24)–(26)*.*
  (c) $T \to +\infty$*,* $E \to E_{\max}(\rho_0)$ *and* $R \to R_{\rho_0}^h$ *(uniformly in* t *on each fixed compact interval) as* $\bar{\rho} \to \rho_0$*.*

(ii) *For all* T *large enough, there exists* $\bar{\rho} \in (d_{\min}, d^*)$ *and a* T*-periodic function* R *satisfying* (21), (22)*,* $E > E_{\max}(\bar{\rho})$ *and the following properties*:
  (a) R *is even in* t*,* $R(t) > 0$ *for all* $t \in [0, T/4)$*,* $R(t + T/2) = -R(t)$ *for all* $t \in \mathbb{R}$*,*
  (b) $\bar{\rho} \to \rho_0$*,* $E \to E_{\max}(\rho_0)$ *and* $R \to R_{\rho_0}^h$ *(uniformly in* t *on each fixed compact interval) as* $T \to +\infty$*.*

For a numerical illustration we consider the case of Morse interaction potentials illustrated by Fig. 6. Fig. 7 shows the solutions period as the energy difference E is varied along the level line Δ_0. The first solution family provided by Theorem 1 (property (i)) corresponds to the left part of the curve. The second solution family (property (ii)) corresponds to a part of the curve at the right of the asymptote where the period T decreases with increasing E. One can notice that T does not vary monotonically as E is further increased along $\Delta_0 \cap \Lambda_o$. For large enough values of T, we find two solutions of (21), (22) having different energies $E > E_{\max}(\bar{\rho})$.

4. Persistence of relative periodic orbits at finite mass ratio

In Section 4.1 we derive a set of nondegeneracy conditions under which $F_{0,\bar{\omega}_0}$ is a submersion at a given periodic solution of the infinite mass ratio problem. Such a solution will be called *normal*, following the terminology introduced in references [37,27] (note that the definition of normal periodic orbits given in these references is more general). This

result will be used in Section 4.2, where we obtain for $\epsilon \approx 0$, $\bar{\omega} \approx \bar{\omega}_0$ a family of periodic solutions of (5) close to the normal periodic solution (this follows from a Lyapunov–Schmidt reduction). This procedure will be applied to the particular solutions of the infinite mass ratio problem obtained in Section 3.

4.1. Conditions for normal degeneracy when $\epsilon = 0$

Let us suppose that (20) has a 1-periodic solution $\bar{u}_0 = (\bar{\varrho}_0, 0)^t, r_2^0$ for $T = T_0$ with an angular velocity $\bar{\omega}_0$. We shall give general conditions under which $F_{0,\bar{\omega}_0}$ is a submersion at the point $(r_1, v_1, r_2, v_2, \bar{\varrho}, T, \alpha, \beta) = X_0$ where $X_0 = (0, \frac{1}{2}\bar{\omega}_0\bar{u}_0^{\perp}, r_2^0, v_2^0, \bar{\varrho}_0, T_0, 0, 0)$ and $T_0^{-1}\dot{r}_2^0 = v_2^0$. We recall that $F_{0,\bar{\omega}_0} : \mathbb{X} \to \mathbb{Y}$ is a submersion at X_0 if $DF_{0,\bar{\omega}_0}(X_0)$ is surjective and its kernel has a closed complement in $\mathbb{X}$. In what follows we prove (under some nondegeneracy conditions) that $DF_{0,\bar{\omega}_0}(X_0)$ is surjective with a finite-dimensional kernel.

Now let us consider $Y = (\underline{a}, \underline{b}, \underline{c}, \underline{d}, e) \in \mathbb{Y}$ and look for a solution $X = (\delta r_1, \delta v_1, \delta r_2, \delta v_2, \delta\bar{\varrho}, \delta T, \alpha, \beta)$ of the equation

$$DF_{0,\bar{\omega}_0}(X_0)X = Y. \tag{42}$$

Eq. (42) reads

$$\begin{aligned}
&\delta\dot{r}_1 - T_0\big(2\delta v_1 - \bar{\omega}_0\delta\bar{u}^{\perp}\big) = \underline{a},\\
&\delta\dot{v}_1 = \beta T_0\underline{u}_0^{\perp} + \underline{b},\\
&\delta\dot{r}_2 - T_0\delta v_2 = T_0\alpha\overline{\mathcal{G}}\big(\bar{u}_0, r_2^0\big) + \delta T v_2^0 + \underline{c},\\
&\delta\dot{v}_2 + T_0 D_{r_2}\overline{\mathcal{G}}\big(\bar{u}_0, r_2^0\big)\delta r_2 + T_0 D_{\bar{u}}\overline{\mathcal{G}}\big(\bar{u}_0, r_2^0\big)\delta\bar{u} = \alpha T_0 v_2^0 - \delta T\overline{\mathcal{G}}\big(\bar{u}_0, r_2^0\big) + \underline{d},
\end{aligned} \tag{43}$$

with the integral equation

$$\begin{aligned}
&\int_0^1 \left(-\frac{1}{2}\bar{\omega}_0^2\bar{u}_0 + \overline{\mathcal{F}}(\bar{u}_0, r_2^0), \delta\bar{u}\right) dt + \int_0^1 \big(\bar{\omega}_0\delta v_1^{\perp}, \bar{u}_0\big)\, dt\\
&\quad + \int_0^1 \big(D_{\bar{u}}\overline{\mathcal{F}}\big(\bar{u}_0, r_2^0\big)\delta\bar{u} + D_{r_2}\overline{\mathcal{F}}\big(\bar{u}_0, r_2^0\big)\delta r_2, \bar{u}_0\big)\, dt = -e,
\end{aligned} \tag{44}$$

where we have noted $\delta\bar{u} = (\delta\bar{\varrho}, 0)^t$. We first consider the resolvent equations for the heavy masses motion:

$$\delta\dot{r}_1 = T_0\big(2\delta v_1 - \bar{\omega}_0\delta\bar{u}^{\perp}\big) + \underline{a}, \tag{45}$$

$$\delta\dot{v}_1 = \beta T_0\bar{u}_0^{\perp} + \underline{b}. \tag{46}$$

Eq. (46) has a 1-periodic solution if $\int_0^1 (\beta T_0\bar{u}_0^{\perp} + \underline{b})\, dt = 0$, which can be splitted into

$$\int_0^1 \big(\underline{b} + \beta T_0\bar{u}_0^{\perp}, \bar{u}_0\big)\, dt = 0, \qquad \int_0^1 \big(\underline{b} + \beta T_0\bar{u}_0^{\perp}, \bar{u}_0^{\perp}\big)\, dt = 0.$$

The first equation is automatically satisfied since $\underline{b} \in \mathbb{L}_0^2$ (this implies $\int_0^1 (\underline{b}(s), \bar{u}_0)\, ds = 0$). In order to satisfy the second equation, we find

$$\beta = -\frac{1}{T_0\|\bar{u}_0\|^2}\int_0^1 \big(\underline{b}, \bar{u}_0^{\perp}\big). \tag{47}$$

This compatibility condition has a simple interpretation. Indeed, for $\epsilon = 0$ and $\bar{u} = \bar{u}_0$, we have $\nabla J = (0, \bar{u}_0^{\perp}, 0, 0)^t$ at $(r_1, v_1, r_2, v_2) = (0, \frac{1}{2}\bar{\omega}_0\bar{u}_0^{\perp}, r_2^0, v_2^0)$ (the rescaled angular momentum J is defined by Eq. (8)). Since J is a conserved quantity of (5), the range of the left side of (43) is L^2-orthogonal to ∇J taken at the basic state (see [37]). This yields precisely the compatibility condition (47).

Integrating (46), we find

$$\delta v_1(t) = \delta v + I_{\underline{b}}(t) \tag{48}$$

where $I_{\underline{b}}$ is the unique primitive of $\underline{b} - \frac{\overline{u_0}^{\perp}}{\|\bar{u}_0\|^2}\int_0^1 (\underline{b}, \bar{u}_0^{\perp})\,dt$ such that $\int_0^1 I_{\underline{b}}(s)\,ds = 0$ and δv denotes an arbitrary constant vector that remains to be determined. Inserting (48) into (45) yields

$$\delta\dot{r}_1 = T_0\big(2\delta v - \bar{\omega}_0\delta\bar{u}^{\perp} + 2I_{\underline{b}}\big) + \underline{a}. \tag{49}$$

Eq. (49) has a 1-periodic solution r_1 if its left side has 0 time-average, i.e.

$$\delta v = \frac{1}{2}\bar{\omega}_0\delta\bar{u}^{\perp} - \int_0^1 \left(I_{\underline{b}}(s) + \frac{\underline{a}(s)}{2T_0}\right) ds. \tag{50}$$

Then δr_1 is uniquely determined by the equations

$$\delta\dot{r}_1 = 2T_0 I_{\underline{b}} + \underline{a} - \int_0^1 \big(2T_0 I_{\underline{b}}(s) + \underline{a}(s)\big)\,ds, \qquad \int_0^1 \delta r_1(s)\,ds = 0. \tag{51}$$

Moreover, we have obtained

$$\delta v_1 = \frac{1}{2}\bar{\omega}_0\delta\bar{u}^{\perp} + \mathcal{I}_1(\underline{a}, \underline{b}) \tag{52}$$

where $\mathcal{I}_1(\underline{a}, \underline{b}) = -\int_0^1 (I_{\underline{b}}(s) + \frac{a(s)}{2T_0})\,ds + I_{\underline{b}}$.

Now we consider the linearized equation for light mass motion coupled with the condition (44). Eliminating δv_2 from the equations and using (20) yields

$$\delta\ddot{r}_2 + T_0^2 D_{r_2}\overline{\mathcal{G}}\big(\bar{u}_0, r_2^0\big)\delta r_2 = -T_0^2 D_{\bar{u}}\overline{\mathcal{G}}\big(\bar{u}_0, r_2^0\big)\delta\bar{u} + \alpha\left(T_0^2 v_2^0 + T_0\frac{d}{dt}\overline{\mathcal{G}}(\bar{u}_0, r_2^0)\right) + \delta T 2\dot{v}_2^0 + \dot{\underline{c}} + T_0\underline{d}, \tag{53}$$

and we have $D_{r_2}\overline{\mathcal{G}}(\bar{u}_0, r_2^0) = D_{r_2}^2 V(\bar{u}_0, r_2^0)$. We have in addition

$$T_0\delta v_2 = \delta\dot{r}_2 - T_0\alpha\overline{\mathcal{G}}\big(\bar{u}_0, r_2^0\big) - \delta T v_2^0 - \underline{c}. \tag{54}$$

Due to the time translation invariance, we know that $\dot{r}_2^0$ lies in the kernel of the operator $\mathcal{L}\colon \mathbb{H}^2 \to \mathbb{L}^2$, $v \mapsto \ddot{v} + T_0^2 D_{r_2}^2 V(\bar{u}_0, r_2^0)v$. We make the following assumption:

Hypothesis 2.

$$\mathcal{K}\mathrm{er}\,\mathcal{L} = \langle\dot{r}_2^0\rangle.$$

This condition will be generically satisfied, because $V(\bar{u}_0, .)$ is not invariant under rotations of r_2 once $\bar{u}_0$ has been fixed. Since $\mathcal{L}$ is a Fredholm operator with index 0 and is self-adjoint, Eq. (53) has a 1-periodic solution if and only if

$$\begin{aligned} -T_0^2\int_0^1 \big(D_{\bar{u}}\overline{\mathcal{G}}\big(\bar{u}_0, r_2^0\big)\delta\bar{u}, \dot{r}_2^0\big)\,dt + \alpha\int_0^1 \left(T_0^2 v_2^0 + T_0\frac{d}{dt}\overline{\mathcal{G}}\big(\bar{u}_0, r_2^0\big), \dot{r}_2^0\right) dt \\ + 2\delta T\int_0^1 \big(\dot{v}_2^0, \dot{r}_2^0\big)\,dt + \int_0^1 \big(\dot{\underline{c}} + T_0\underline{d}, \dot{r}_2^0\big)\,dt = 0. \end{aligned} \tag{55}$$

Since $\overline{\mathcal{G}} = \nabla_{r_2} V$ we have automatically

$$\int_0^1 \big(D_{\bar{u}}\overline{\mathcal{G}}\big(\bar{u}_0, r_2^0(s)\big)\delta\bar{u}, \dot{r}_2^0(s)\big)\,ds = 0.$$

Moreover, we have also $\int_0^1 (\dot{v}_2^0, \dot{r}_2^0)\,dt = T_0 \int_0^1 (\dot{v}_2^0, v_2^0) = 0$. Consequently, the compatibility condition (55) yields (integrate by parts)

$$\alpha = -\frac{\int_0^1 [(\underline{d}, v_2^0) + (\underline{c}, \overline{\mathcal{G}}(\bar{u}_0, r_2^0))]\,ds}{T_0 \int_0^1 [\|v_2^0(s)\|^2 + \|\overline{\mathcal{G}}(\bar{u}_0, r_2^0)(s)\|^2]\,ds}, \tag{56}$$

or equivalently (use (20))

$$\alpha = \frac{\int_0^1 [(\underline{c}, \dot{v}_2^0) - T_0(\underline{d}, v_2^0)]\,ds}{\int_0^1 [T_0^2\|v_2^0(s)\|^2 + \|\dot{v}_2^0\|^2]\,ds}.$$

As previously this compatibility condition has a simple interpretation. For $\epsilon = 0$ and $\bar{u} = \bar{u}_0$, we have at $(r_1, v_1, r_2, v_2) = (0, \frac{1}{2}\bar{\omega}_0\bar{u}_0^{\perp}, r_2^0, v_2^0)$ the equality $\nabla H = (0, 0, \overline{\mathcal{G}}(\bar{u}_0, r_2^0), v_2^0)^t$. Since H is a conserved quantity of (5), the range of the left side of (43) is L^2-orthogonal to ∇H taken at the basic state, which yields the compatibility condition (56).

Now let us solve Eq. (53). For this purpose we split the right side into three parts. We consider a 1-periodic solution k_2^0 of

$$\ddot{k}_2^0 + T_0^2 D_{r_2}\overline{\mathcal{G}}(\bar{u}_0, r_2^0)k_2^0 = 2\dot{v}_2^0. \tag{57}$$

We also consider a 1-periodic solution h_2^0 of

$$\ddot{h}_2^0 + T_0^2 D_{r_2}\overline{\mathcal{G}}(\bar{u}_0, r_2^0)h_2^0 = -T_0^2 D_{\bar{u}}\overline{\mathcal{G}}(\bar{u}_0, r_2^0)\bar{u}_0. \tag{58}$$

Moreover, with α given by (56), we note $\mathcal{I}_2(\underline{c}, \underline{d})$ the 1-periodic solution of

$$\delta\ddot{r}_2 + T_0^2 D_{r_2}\overline{\mathcal{G}}(\bar{u}_0, r_2^0)\delta r_2 = \alpha\left(T_0^2 v_2^0 + T_0\frac{d}{dt}\overline{\mathcal{G}}(\bar{u}_0, r_2^0)\right) + \dot{\underline{c}} + T_0\underline{d} \tag{59}$$

fixed by the condition $\int_0^1 (\mathcal{I}_2(\underline{c}, \underline{d}), \dot{r}_2^0)\,dt = 0$.

Setting $\delta\bar{u} = \mu_1\bar{u}_0$, the solutions of (53) take the form

$$\delta r_2 = \lambda\dot{r}_2^0 + \mu_1 h_2^0 + \delta T k_2^0 + \mathcal{I}_2(\underline{c}, \underline{d}), \tag{60}$$

where λ is an arbitrary constant.

Now there remains to solve the integral equation (44). Inserting the solutions (52), (60) into (44) and using (20), one obtains

$$\delta T\int_0^1 \big(D_{r_2}\overline{\mathcal{F}}(\bar{u}_0, r_2^0)k_2^0, \bar{u}_0\big)\,dt + \mu_1\Delta_1 = -e - \int_0^1 \big(D_{r_2}\overline{\mathcal{F}}(\bar{u}_0, r_2^0)\mathcal{I}_2(\underline{c}, \underline{d})\,dt + \bar{\omega}_0\mathcal{I}_1^{\perp}(\underline{a}, \underline{b}), \bar{u}_0\big)\,dt, \tag{61}$$

with

$$\Delta_1 = \int_0^1 \big(D_{\bar{u}}\overline{\mathcal{F}}(\bar{u}_0, r_2^0)\bar{u}_0 + D_{r_2}\overline{\mathcal{F}}(\bar{u}_0, r_2^0)h_2^0, \bar{u}_0\big)\,dt - \frac{\bar{\omega}_0^2}{2}\bar{\varrho}_0^2. \tag{62}$$

Note that the value of Δ_1 is independent of the choice of h_2^0 (defined up to an element of $\mathcal{K}\mathrm{er}\,\mathcal{L}$). We make the following assumption.

Hypothesis 3. The coefficient Δ_1 defined by (62) does not vanish.

Since $\Delta_1 \neq 0$, Eq. (61) can be solved with respect to μ_1, which determines $\delta\bar{u} = \mu_1\bar{u}_0$ and $\delta\bar{\varrho} = \mu_1\bar{\varrho}_0$. As a conclusion, we have proved that (42) admits solutions X for all $Y \in \mathbb{Y}$, i.e. $DF_{0,\bar{\omega}_0}(X_0)$ is surjective. Putting together equations (47), (56), (51), (61), (52), (60) and (54), a unique solution $X = (\delta r_1, \delta v_1, \delta r_2, \delta v_2, \delta\bar{\varrho}, \delta T, \alpha, \beta)$ is fixed by the choice of Y and the two arbitrary parameters λ, δT. The kernel of $DF_{0,\bar{\omega}_0}(X_0)$ is therefore two-dimensional and spanned by the vectors $(\delta r_1, \delta v_1, \delta r_2, \delta v_2, \delta\bar{\varrho}, \delta T, \alpha, \beta) = V_1, V_2$ (corresponding respectively to $\lambda = 1, \delta T = 0$ and $\lambda = 0, \delta T = 1$) given by

$$V_1 = \big(0, 0, \dot r_2^0, T_0^{-1}\ddot r_2^0, 0, 0, 0, 0\big), \tag{63}$$

$$V_2 = \left(0, \frac{1}{2}\bar\omega_0\mu_1^*\bar u_0^\perp, \mu_1^* h_2^0 + k_2^0, T_0^{-1}\big[\mu_1^*\dot h_2^0 + \dot k_2^0 - v_2^0\big], \mu_1^*\bar\varrho_0, 1, 0, 0\right), \tag{64}$$

where $\mu_1^* = -\Delta_1^{-1}\int_0^1 (D_{r_2}\overline{\mathcal F}(\bar u_0, r_2^0)k_2^0, \bar u_0)\,dt$.

As a conclusion, we have shown that $F_{0,\bar\omega_0}$ is a submersion at $X = X_0$. We sum up our result in the following lemma.

Lemma 2. *Assume problem* (20) *has a* 1*-periodic solution* $\bar u_0 = (\bar\varrho_0, 0)^t$, r_2^0 (*different from an equilibrium*) *for* $T = T_0$ *and* $\bar\omega = \bar\omega_0$. *If the nondegeneracy Hypotheses* 2, 3 *are satisfied, then* $F_{0,\bar\omega_0}$ *is a submersion at the point* $(r_1, v_1, r_2, v_2, \bar\varrho, T, \alpha, \beta) = X_0$ *where* $X_0 = (0, \frac{1}{2}\bar\omega_0\bar u_0^\perp, r_2^0, v_2^0, \bar\varrho_0, T_0, 0, 0)$ *and* $T_0^{-1}\dot r_2^0 = v_2^0$. *Moreover, the kernel of* $DF_{0,\bar\omega_0}(X_0)$ *is two-dimensional.*

4.2. Zero set of $F_{\epsilon,\bar\omega}$*: local structure and associated time-periodic solutions*

Given a solution $X_0 = (0, \frac{1}{2}\bar\omega_0\bar u_0^\perp, r_2^0, v_2^0, \bar\varrho_0, T_0, 0, 0)$ of $F_{0,\bar\omega_0}(X_0) = 0$ satisfying the nondegeneracy Hypotheses 2 and 3, we have shown that $DF_{0,\bar\omega_0}(X_0)$ is surjective with a two-dimensional kernel. Consequently, by the implicit function theorem (just using the classical Lyapunov–Schmidt decomposition) the zero set $F_{0,\bar\omega_0}^{-1}(0)$ is locally a two-dimensional submanifold of $\mathbb{X}$. Moreover, the zero set $F_{\epsilon,\bar\omega}^{-1}(0)$ is locally a two-dimensional submanifold for $\epsilon \approx 0$ and $\bar\omega \approx \bar\omega_0$, since $F_{\epsilon,\bar\omega}$ is a small C^1 perturbation of $F_{0,\bar\omega_0}$.

These properties can be reformulated as follows. There exist neighborhoods Ω of X_0 in $\mathbb{X}$, Λ of $(0, \bar\omega_0)$ in $\mathbb{R}^2$ and $\mathcal{V}$ of $(0, 0)$ in $\mathbb{R}^2$, and a C^k map $\Phi : \mathcal{V}\times\Lambda \to \mathbb{X}$, such that for all $(\epsilon, \bar\omega) \in \Lambda$, the solutions $X \in \Omega$ of $F_{\epsilon,\bar\omega}(X) = 0$ take the form

$$X = X_0 + \lambda V_1 + \delta T V_2 + \Phi(\lambda, \delta T, \epsilon, \bar\omega), \quad (\lambda, \delta T) \in \mathcal{V}, \tag{65}$$

where V_1, V_2 are the eigenvectors of $DF_{0,\bar\omega_0}(X_0)$ given by (63), (64). We have in addition $\Phi(0, 0, 0, \bar\omega_0) = 0$ and $D_{(\lambda,\delta T)}\Phi(0, 0, 0, \bar\omega_0) = 0$. Note that the first component of X is $\mathrm{O}(|\epsilon|)$ (system (19) implies $r_1 = 0$). Moreover, varying the parameter λ simply corresponds to a phase shift.

By construction, zeros $X = (r_1, v_1, r_2, v_2, \bar\varrho, T, \alpha, \beta)$ of $F_{\epsilon,\bar\omega}$ provide 1-periodic solutions $u = (r_1, v_1, r_2, v_2)^t$ of (9), (10). Considering the basic state X_0, if $\bar\varrho_0 \neq 0$ and r_2^0 is not an equilibrium solution of (20) then $\nabla J(u)$, $\nabla H(u)$ do not vanish and are not colinear. Consequently, the assumptions of Proposition 1 are satisfied when $u = (r_1, v_1, r_2, v_2)^t$ is derived from a perturbed solution X with δT, ϵ sufficiently small in (65). It follows that $\alpha = \beta = 0$ and $\tilde u(t) = u(t/T)$ is a T-periodic solution of the conservative system (4), (5).

Consequently, we have obtained (for $\epsilon \approx 0$ and $\bar\omega \approx \bar\omega_0$) a two-parameter family of time-periodic solutions of (4), (5) with $\bar u = (\bar\varrho, 0)^t$, close to a given solution $(r_1, v_1, r_2, v_2, \bar u) = (0, \frac{1}{2}\bar\omega_0\bar u_0^\perp, r_2^0(t/T_0), v_2^0(t/T_0), (\bar\varrho_0, 0)^t)$ with period $T = T_0$, assumed to exist for $\epsilon = 0$, $\bar\omega = \bar\omega_0$ and satisfying some nondegeneracy assumptions. The family of solutions is parametrized by phase (corresponding to parameter λ) and period $T \approx T_0$ (corresponding to parameter δT). Relaxing the restriction on $\bar u$ (i.e. allowing nonvanishing second components) one obtains a three-parameter family of solutions of (4), (5), thanks to the invariance of the system under rotations. This in turn provides a three-parameter family of time-periodic solutions for the Hamiltonian system (3) for $\epsilon \approx 0$ ($\epsilon \neq 0$) and $\bar\omega \approx \bar\omega_0$.

We sum up this result in the following theorem (we denote by $\langle u_1\rangle$ the time-average of u_1).

Theorem 2. *Fix* $\epsilon = 0$, $\bar\omega = \bar\omega_0$ *in* (4)–(5)–(14) *and consider a* T_0*-periodic solution* $(r_1, v_1, r_2, v_2, \bar u) = U_0$ *different from an equilibrium. If the nondegeneracy Hypotheses* 2, 3 *are satisfied, then* U_0 *belongs to a local three-parameter family of solutions of* (4)–(5)–(14) (*for* $\epsilon = 0$, $\bar\omega = \bar\omega_0$), *parametrized by phase, rotational degree of freedom, and period* $T \approx T_0$. *This family of solutions persists for* $\epsilon \approx 0$ (*large mass ratio limit*) *and* $\bar\omega \approx \bar\omega_0$ (*nearby angular velocities*). *For* $\epsilon \neq 0$, *the corresponding solutions of the Hamiltonian system* (3) *satisfy* $u_1 - \langle u_1\rangle = \mathrm{O}(\epsilon^2)$, *with oscillations principally localized on the* u_2*-component as* $\epsilon \approx 0$. *They correspond to relative periodic orbits of system* (1) *with* $\gamma = \epsilon^{-2}$, *time-periodic in a frame rotating at velocity* $\epsilon\bar\omega$.

Moreover, using Theorems 1 and 2 in conjunction provides a global branch of periodic solutions of (4)–(5)–(14) (we state this result below in Theorem 3). This family of solutions is parametrized by period T, mass ratio ϵ and

angular velocity $\bar{\omega}$ (in addition to phase shift, rotational degree of freedom). The solution branch is global in the sense that period T is unbounded along it, but it remains only local in transverse directions since we are restricted to small values of ϵ and $\bar{\omega}$.

Theorem 3. *Assume the hypothesis of Theorem* 1 *are satisfied, and consider a* T_0*-periodic* (*nonconstant*) *solution* $(R, \bar{\rho})$ *of* (21), (22) *in the global branch of solutions provided by Theorem* 1. *Consider the* T_0*-periodic solution* U_0 *of* (4)–(5)–(14) *with* $\epsilon = 0$, $\bar{\omega} = 0$, *defined by* $(r_1, v_1, r_2, v_2, \bar{u}) = U_0$ *and* $\bar{u} = (2\bar{\rho}, 0)^t$, $r_1 = v_1 = 0$, $r_2(t) = (0, R(t))^t$, $T_0^{-1}\dot{r}_2 = v_2$. *Consider a* (*generic*) *choice of solution* $(R, \bar{\rho})$ *such that Hypotheses* 2, 3 *are satisfied* (*this is the case in particular if one considers in Theorem* 1(i) *a solution sufficiently close to the triangular equilibrium,* ρ^* *is not a multiple of* R^* *and the coefficient* $h(\rho^*)$ *defined by* (27) *does not vanish*). *Then* U_0 *belongs to a local family of solutions of* (4)–(5)–(14), *parametrized by phase, rotational degree of freedom, period* $T \approx T_0$, $\epsilon \approx 0$ *and* $\bar{\omega} \approx 0$. *For* $\epsilon \neq 0$, *the corresponding solutions of the Hamiltonian system* (3) *satisfy* $u_1 - \langle u_1 \rangle = \mathrm{O}(\epsilon^2)$, *with oscillations principally localized on the* u_2*-component as* $\epsilon \approx 0$. *They correspond to relative periodic orbits of system* (1) *with* $\gamma = \epsilon^{-2}$, *time-periodic in a frame rotating at velocity* $\epsilon\bar{\omega}$.

As indicated in Theorem 3, the (generically satisfied) conditions described in Hypotheses 2, 3 are satisfied if one considers in Theorem 1 (property (i)) a solution sufficiently close to the triangular equilibrium, $\rho^*/R^* \notin \mathbb{N}$ and the coefficient $h(\rho^*)$ defined by (27) does not vanish. This property is checked in Appendix A using classical arguments of perturbation theory.

5. Numerical continuation of relative periodic orbits

In this section we numerically illustrate Theorems 2 and 3, which ensure that (generic) relative periodic orbits existing in our triatomic system for $\epsilon = 0$ and a given rescaled angular velocity $\bar{\omega} = \bar{\omega}_0$ can be smoothly continued to $\epsilon \approx 0$ and $\bar{\omega} \approx \bar{\omega}_0$. Moreover we shall qualitatively describe (for some solutions provided by Theorem 3) how the oscillations evolve with increasing $\bar{\omega}$, and we shall study their stability properties.

We choose to fix the period T of solutions and perform the continuation in two steps. Firstly we set $\bar{\omega} = 0$ and obtain a family of solutions by varying ϵ. Secondly, for different fixed values of ϵ we continue the periodic solutions with respect to $\bar{\omega}$.

In what follows we briefly describe our numerical method (more details and references on the numerical continuation of periodic solutions in conservative systems can be found in [7,20]). As a starting point in the case $\epsilon = 0$ and $\bar{\omega} = 0$ we choose one of the solutions found in Section 3.2.2, where the system has an isosceles configuration. Then the computation of other periodic solutions for different values of $(\epsilon, \bar{\omega})$ is based on path-following and the Newton method to find fixed points of the time-T map φ_T of the flow (the dynamical equations are integrated with a standard Runge Kutta method). The Newton method is carried out in different ways when $\bar{\omega} = 0$ and $\bar{w} \neq 0$.

During the continuation with respect to ϵ ($\bar{\omega} = 0$ being fixed), the system keeps an isosceles configuration. Consequently one has to continue a (reversible) periodic solution (R, R', ρ, ρ') of a 4-dimensional reversible differential equation, where ρ is the half distance between the two heavy atoms B and R is the coordinate of the light atom A on the perpendicular axis to the B–B line (see Fig. 2). Setting $\bar{u} + \epsilon r_1(t) = (2\rho(t), 0)^t$ ($\rho > 0$) and $r_2(t) = (0, R(t))^t$ in Eq. (5), one obtains the differential system

$$\begin{aligned}
\rho'' &= -\epsilon^2\left(U'(2\rho) + W'\big(\sqrt{R^2+\rho^2}\big)\frac{\rho}{\sqrt{R^2+\rho^2}}\right),\\
R'' &= -\big(2+\epsilon^2\big)W'\big(\sqrt{R^2+\rho^2}\big)\frac{R}{\sqrt{R^2+\rho^2}}.
\end{aligned} \tag{66}$$

Time-periodic and reversible solutions are deduced from the fixed points of the map

$$\begin{aligned}
&\big(R(0), \rho(0)\big) \mapsto \big(R(T), \rho(T)\big),\\
&\big(R(T), R'(T), \rho(T), \rho'(T)\big) = \varphi_T\big(R(0), 0, \rho(0), 0\big)
\end{aligned}$$

(see [20], Appendix A.1 for more details).

The continuation with respect to $\bar{w}$ for a fixed ϵ is more involved because the isosceles configuration is lost when $\bar{w} \neq 0$ and we have to deal with the full 8-dimensional differential system (5). In that case, the Newton method has to be adapted because the linearized map $I - D\varphi_T$ is not invertible at any fixed point of φ_T (this originates from the invariance of (5) under rotations and time-shift). At each step of the numerical continuation, we partially invert $I - D\varphi_T$ with a Singular Value Decomposition (which is equivalent to fixing some phase conditions). The same partial inverse is used for *all* the iterations of the Newton method to accelerate the numerical computations. Moreover, we use a numerical derivative to compute $D\varphi_T$ instead of integrating the linearized dynamical equations (this yields more accurate results).

Now let us start with a continuation with respect to ϵ, keeping $\bar{\omega} = 0$. As a starting point in the case $\epsilon = 0$ we choose an oscillatory motion of the light atom corresponding to an "inversion" (see Theorem 1, property (ii)). During one oscillation period, this atom crosses twice the segment formed by the two heavy atoms. Most of our numerical results will concern the continuation of this solution with respect to ϵ and $\bar{\omega}$. The present numerical study is not exhaustive, and one could obviously consider the other family of periodic solutions corresponding to nonlinear normal modes of the triangular equilibria (Theorem 1, property (i)), as well as more general periodic solutions existing for $\epsilon = 0$.

As in Section 3.2.2 (Figs. 6 and 7) we consider the interaction potentials $U(x) = W(x) = \frac{1}{2}(e^{-(x-1)} - 1)^2$. Our starting point is the solution with period $T = 15$ and the higher energy difference E with respect to the ground state (see Fig. 7). We shall denote this solution by $(R, \rho) = (R_0(t), \bar{\rho}_0)$, R_0 being T-periodic and $\bar{\rho}_0$ constant. For $\epsilon = 0$, $(R_0, \bar{\rho}_0)$ defines a solution of (66) which can be continued at least to small values of ϵ according to Theorem 3.

Numerically we manage to make the continuation up to $\epsilon = 0.4$, and after this point the periodic solution is too unstable to be computed with a good accuracy. We have computed the Floquet spectrum of the periodic solutions as ϵ is varied along the solution branch. In addition to a double non-semi-simple eigenvalue at $+1$ there is a symmetric pair of eigenvalues depending on ϵ. This pair lies on the unit circle for small enough ϵ and collides at $+1$ for $\epsilon \approx 0.23$. Then it becomes real positive as ϵ is further increased, and moves away from the unit circle at least up to $\epsilon = 0.4$, the end of the numerical continuation.

In the sequel we note $\tilde{H}_\epsilon$ the Hamiltonian (1) in order to stress its dependency in ϵ. Similarly we shall note H_ϵ the reduced Hamiltonian (3) and we recall $H_\epsilon = \tilde{H}_\epsilon - \Omega \tilde{J}$. The above solutions satisfy $\tilde{J} = 0$ and $\tilde{H}_\epsilon = H_\epsilon = \epsilon^{-2}\rho'^2 + (2+\epsilon^2)^{-1}R'^2 + U(2\rho) + 2W(\sqrt{R^2+\rho^2})$. In Fig. 8 (left) we plot the Hamiltonian $\tilde{H}_\epsilon$ as ϵ is varied along the solution branch.

It is worthwhile stressing that the continuation with respect to ϵ can be performed far from the regime $\epsilon \approx 0$ for certain solutions. For example, Fig. 8 (bottom) shows the continuation of a nonlinear normal mode of a triangular equilibrium, from $\epsilon = 0$ (Theorem 1, property (i)) up to $\epsilon = 1$ (in that case all atoms become identical).

Now we continue with respect to $\bar{\omega}$ some of the solutions found previously. This leads us to consider the full 8-dimensional differential system with Hamiltonian H_ϵ defined by (3). Therefore the equations of motion are considered in a frame rotating at angular velocity $\epsilon\bar{\omega}$, and we describe mass positions using the Jacobi coordinates u_1, u_2 described in Fig. 1. We choose to continue two stable solutions for $\bar{\omega} = 0$, corresponding to $\epsilon = 0.1$ and $\epsilon = 0.2$.

In Fig. 9 we plot the Hamiltonian $\tilde{H}_\epsilon$ as ϵ is kept fixed and $\bar{\omega}$ is varied along each solution branch. The turning points (at critical values of $\bar{\omega}$ close to 0.6) correspond to a saddle-center bifurcation of T-periodic solutions. Moreover the endpoints of our numerical continuation correspond to parameter values at which our Newton method does not converge (this occurs when periodic orbits become highly unstable). We detect a second turning point for $\epsilon = 0.2$ but we manage to follow the solution branch only for very small parameter changes after this point. For $\epsilon = 0.2$, periodic orbits near the end of the continuation are similar (up to a change of scale) to the orbit depicted in Fig. 15 for $\bar{\omega} = 0.487$.

By computing the Floquet spectrum of periodic solutions (both for $\epsilon = 0.1$ and $\epsilon = 0.2$) we find the higher energy branch (see Fig. 9) to be unstable at least close to the first turning point, and the lower branch is linearly stable. A pair of Floquet multipliers collides at $+1$ at the turning point.

The saddle-center bifurcations of periodic solutions at $\bar{\omega} \approx 0.6$ can be related to a bifurcation of the same type for relative equilibria. As Fig. 10 shows (for $\epsilon = 0.1$), at $\bar{\omega} = \bar{\omega}_c \approx 0.49$ a symmetric pair of isosceles triangular relative equilibria bifurcates from a linear configuration with $R = 0$ (the family of linear relative equilibria is shown in Fig. 11). We recall the notations $u_1 = (2\rho, 0)^t$ and $u_2 = (0, R)^t$. In parallel, following the initial isosceles triangular configurations (with $R = \pm\sqrt{3}/2$ if $\bar{\omega} = 0$), one can see that $|R|$ decreases as $\bar{\omega}$ is increased. The two families of triangular configurations merge and disappear in a saddle-center bifurcation as $\bar{\omega}$ reaches a critical value close to 0.6

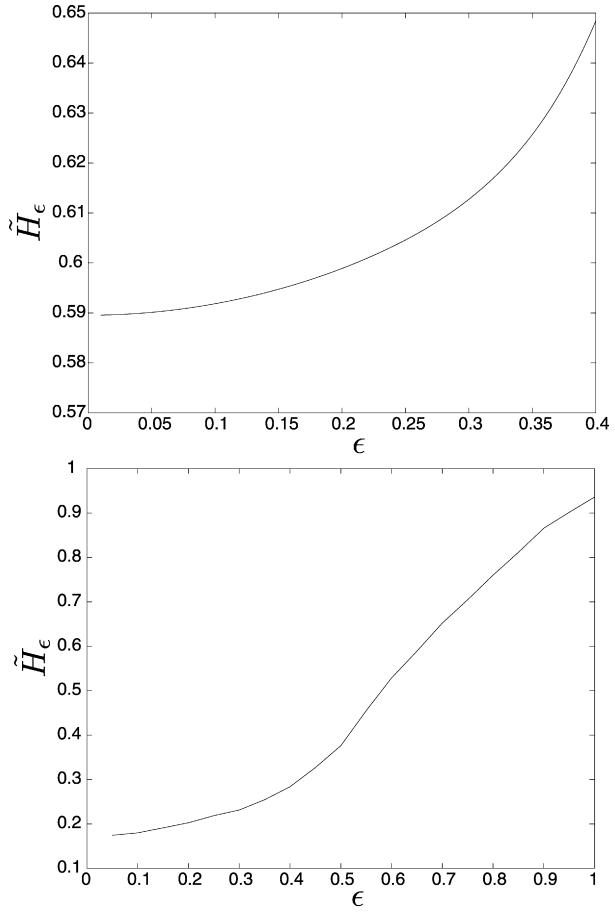

Fig. 8. Top figure: Hamiltonian $\tilde{H}_\epsilon$ versus mass ratio ϵ as the solution $(R_0, \bar{\rho}_0)$ of (66) defined in the text for $\epsilon = 0$ is continued with respect to ϵ. We manage to make the continuation up to $\epsilon = 0.4$. Bottom figure: continuation of the nonlinear normal mode with $T = 6$ provided by Theorem 1, property (i) (see Fig. 7). In the figure the continuation stops at $\epsilon = 1$, but a continuation beyond this value is possible.

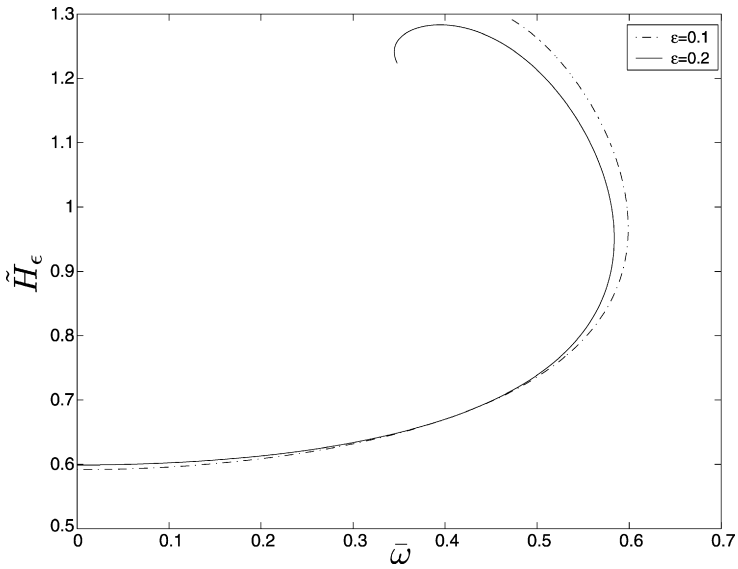

Fig. 9. Hamiltonian $\tilde{H}_\epsilon$ for $\epsilon = 0.1$ (dashed line) and $\epsilon = 0.2$ (continuous line), as $\bar{\omega}$ is varied along each solution branch.

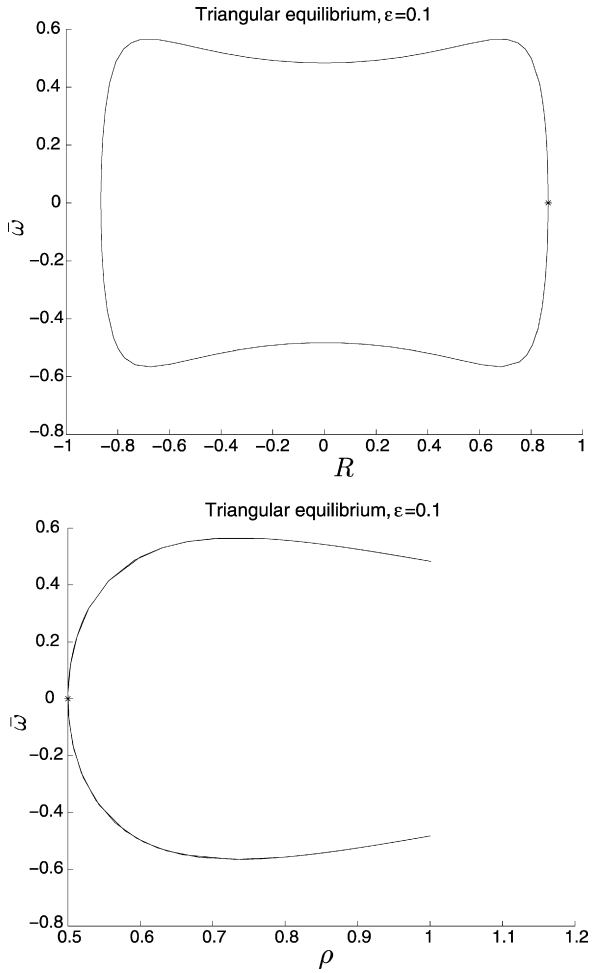

Fig. 10. Family of relative equilibria with $u_1 = (2\rho, 0)^t$ and $u_2 = (0, R)^t$ emanating from an isosceles equilibrium ($R = \pm\sqrt{3}/2$, $\rho = 1/2$) as $\bar{\omega}$ is increased, for $\epsilon = 0.1$. The computations have been performed using the continuation software CL_MATCONT [6].

(see Fig. 10, top). This critical value is very close to a value of $\bar{\omega}$ corresponding to turning points in Fig. 9. This is not surprising, because the bifurcation of relative equilibria are expected to influence the surrounding periodic orbits.

In the same way, the pitchfork bifurcation of relative equilibria at $\bar{\omega} = \bar{\omega}_c$ has also a qualitative effect on the branches of T-periodic solutions. This can be visualized by considering the reduced Hamiltonian H_ϵ as $\bar{\omega}$ is varied along the two branches of T-periodic solutions (Fig. 12). One can see that solution branches are folded, their two parts being very close at a value of $\bar{\omega}$ close to $\bar{\omega}_c$ when ϵ is small.

Now let us describe the influence of the angular velocity on the geometry of periodic solutions. We represent the trajectories in the rotating coordinate system with Jacobi coordinates (Fig. 1) and note $u_1 = \bar{u} + (r_x, r_y)$, $u_2 = (R_x, R_y)$. For $\epsilon = 0.2$, trajectories of T-periodic solutions are represented in Figs. 13–15 for different values of $\bar{\omega}$.

In Fig. 13 one can observe that the isosceles configuration existing for $\bar{\omega} = 0$ ($R_x = 0$) is lost for $\bar{\omega} \neq 0$. The evenness of solutions in t is lost at the same time. For stable solutions, the angular oscillations of the light atom A increase in amplitude as $\bar{\omega}$ increases (see Figs. 13 and 14, right). Despite the loss of evenness in t, trajectories remain invariant under the reflexion $R_x \to -R_x$ and $r_y \to -r_y$, which corresponds to a reversibility symmetry for system (5). More precisely (if a small rotation is applied to make $\bar{u}$ horizontal) the trajectories satisfy $(u_1(t), u_2(t)) = (-Su_1(-t), Su_2(-t))$, where $S(a, b) = (-a, b)$. The solutions obtained by continuation with respect to $\bar{\omega}$ possess this additional symmetry because system (5) is reversible *and* the solutions used to start the continuation are themselves symmetric. Note that for different parameter values one can observe a pitchfork bifurcation breaking this symmetry during the continuation.

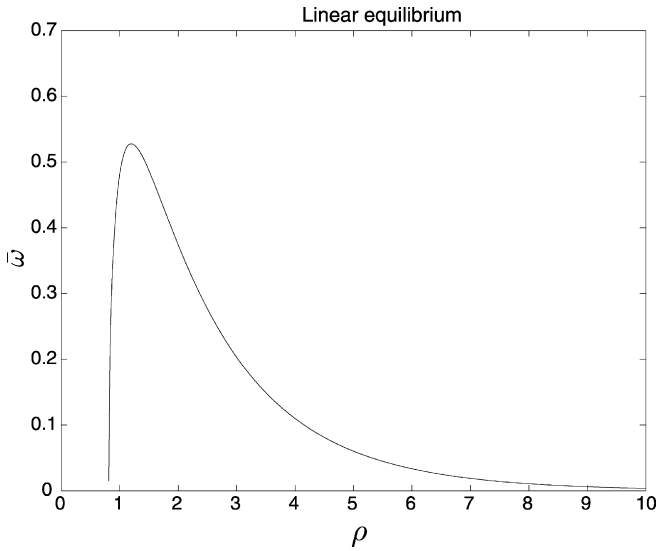

Fig. 11. Family of linear relative equilibria with $u_1 = (2\rho, 0)^t$ and $u_2 = 0$ as $\bar{\omega}$ is varied, for $\epsilon = 0.1$.

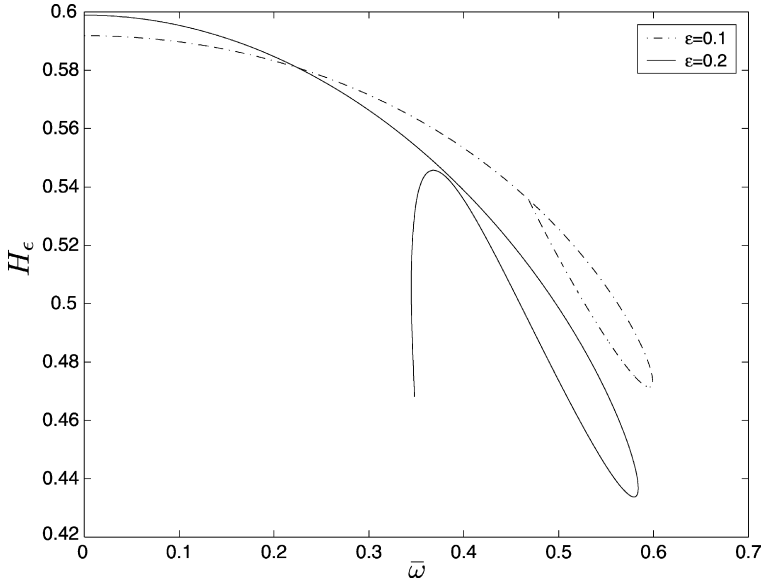

Fig. 12. Reduced Hamiltonian $H_\epsilon = \tilde{H}_\epsilon - \Omega \tilde{J}$ for $\epsilon = 0.1$ (dashed line) and $\epsilon = 0.2$ (continuous line), as $\bar{\omega}$ is varied along the two branches of T-periodic solutions.

On the contrary, on the unstable solution branch the angular oscillations of the light atom A decrease in amplitude as $\bar{\omega}$ increases (see Fig. 15, right). One can observe that the mean B–B stretch $\|\bar{u}\|$ is larger on the unstable solution branch than on the stable one, each of them having a bond length comparable to linear and triangular relative equilibria respectively (compare $\|\bar{u}\|$ in Figs. 14 and 15 with 2ρ in Figs. 10 and 11). At sufficiently small angular velocity, there is also a topological change of the unstable trajectories. In Fig. 15, for $\bar{\omega} = 0.487$, the upper and lower loops of the trajectories are absent in the right plot and new loops appear in the left plot. This phenomenon might be linked with the previously mentioned pitchfork bifurcation of relative equilibria at $\bar{\omega} \approx 0.49$.

We end up our numerical study with some dynamical considerations. For $\epsilon = 0.2$ and $\bar{\omega} = 0.4869$ we perturb the unstable T-periodic solution (choosing a small perturbation close to its unstable manifold) and see how the system evolves with time. In Fig. 16 (left) one can see that this perturbation leads to a partial dissociation of the triatomic

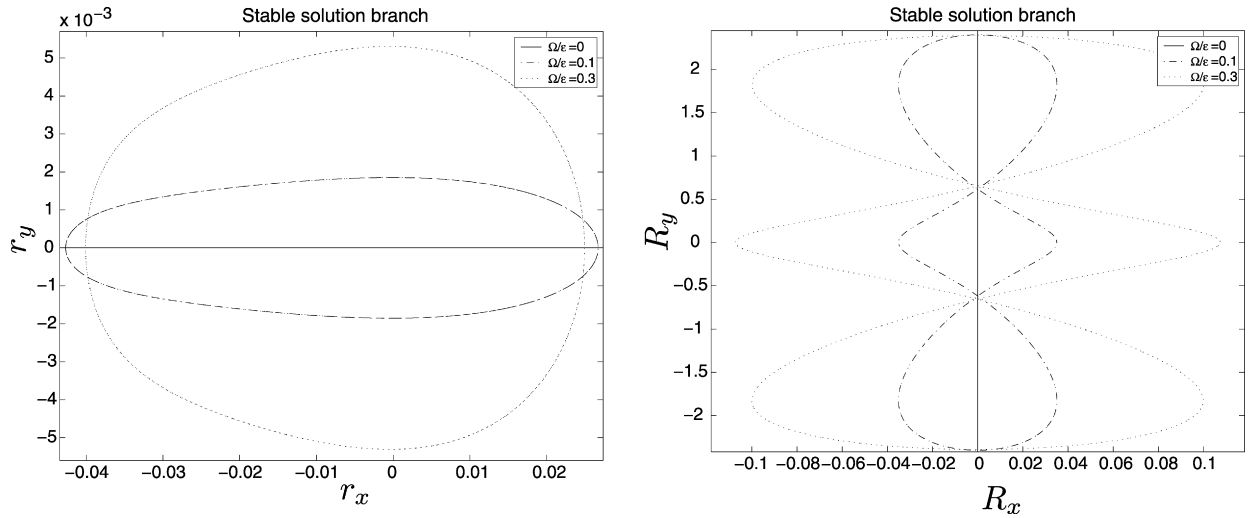

Fig. 13. Time-periodic trajectories corresponding to solutions of Fig. 9, for $\epsilon = 0.2$ and angular velocities $\bar{\omega} = 0$ (full line), $\bar{\omega} = 0.1$ (dashed line), $\bar{\omega} = 0.3$ (dotted line). Right figure: trajectory of the light atom A described by the Jacobi coordinate $u_2 = (R_x, R_y)$. Left figure: variations of the segment between heavy atoms B (Jacobi coordinate u_1). One represents the deviation (r_x, r_y) of the B–B segment with respect to its mean value $\bar{u}$. The mean value for each angular velocity is respectively $\bar{u} = (1.097, 0)$, $\bar{u} = (1.103, -4.2e-6)$, $\bar{u} = (1.154, -4.5e-5)$. Note the small length scale on the r_y axis.

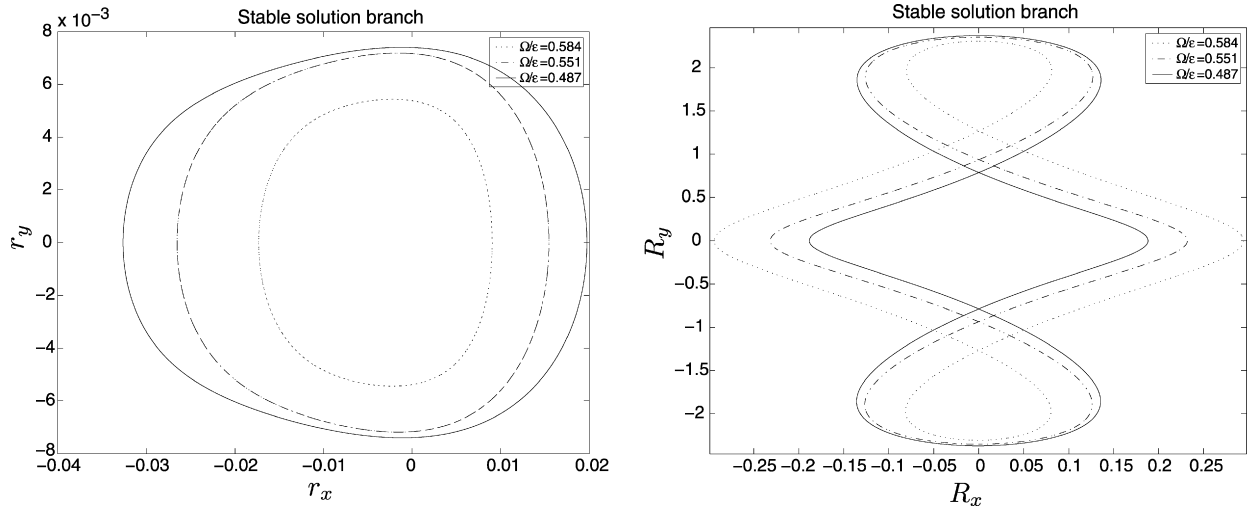

Fig. 14. Time-periodic trajectories corresponding to solutions of Fig. 9, for $\epsilon = 0.2$ and angular velocities $\bar{\omega} = 0.584$ (dotted line), $\bar{\omega} = 0.551$ (dashed line), $\bar{\omega} = 0.487$ (full line). Solutions correspond to the lower-energy (stable) solution branch. The choice of coordinates is the same as in Fig. 13. The mean value of the B–B vector for each angular velocity is respectively $\bar{u} = (1.66, -3.95e-4)$, $\bar{u} = (1.42, -2.47e-4)$, $\bar{u} = (1.29, -1.56e-4)$. Note the small length scale on the r_y axis.

system, where the light atom A remains attached to an heavy atom B and the remaining atom B is ejected. Note that all atomic bonds have the same dissociation energy with our choice of potential V.

Fig. 16 (right) also shows the vertical component of u_2 for a perturbation of the linearly stable solution (applied in the same direction as previously), for an initial perturbation of $\tilde{H}_\epsilon$ lower that 5 percent. The time of integration extends over 40 periods of the unperturbed periodic solution (with period $T = 15$). One can see that the motion of inversion persists, although time-periodic oscillations are replaced by a chaotic regime. This illustrates that these periodic inversions are not stable at the nonlinear level, but nevertheless contribute to organize the dynamics.

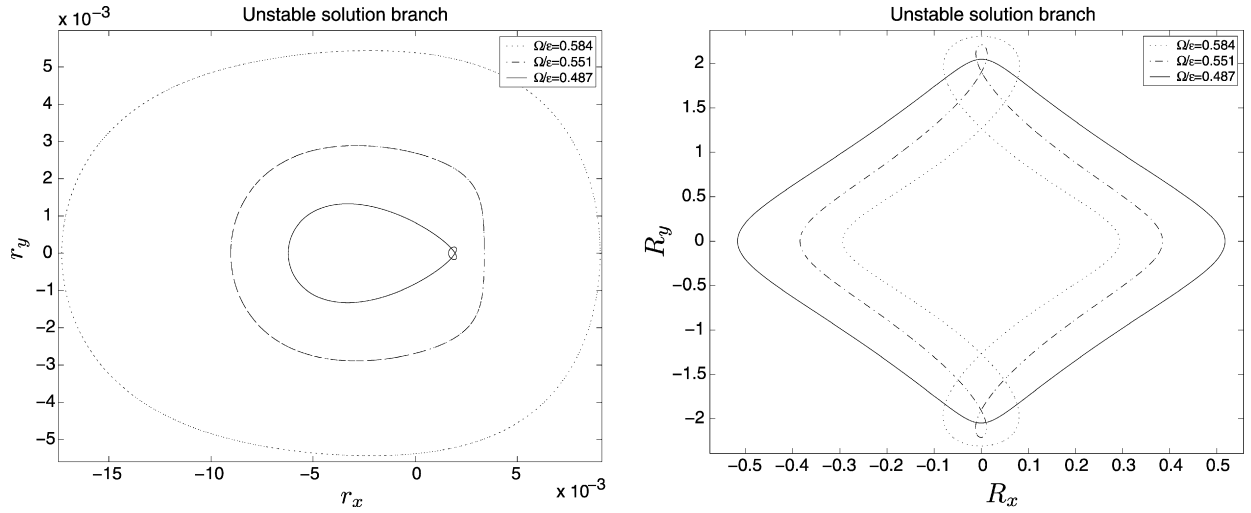

Fig. 15. Time-periodic trajectories corresponding to solutions of Fig. 9, for $\epsilon = 0.2$ and angular velocities $\bar{\omega} = 0.584$ (dotted line), $\bar{\omega} = 0.551$ (dashed line), $\bar{\omega} = 0.487$ (full line). Solutions correspond to the higher-energy (unstable) solution branch. The choice of coordinates is the same as in Fig. 13. The mean value of the B–B vector for each angular velocity is respectively $\bar{u} = (1.66, -3.95e-4)$, $\bar{u} = (2.02, -4.49e-4)$, $\bar{u} = (2.42, -5.01e-4)$. Note the small length scale used on the r_x and r_y axes.

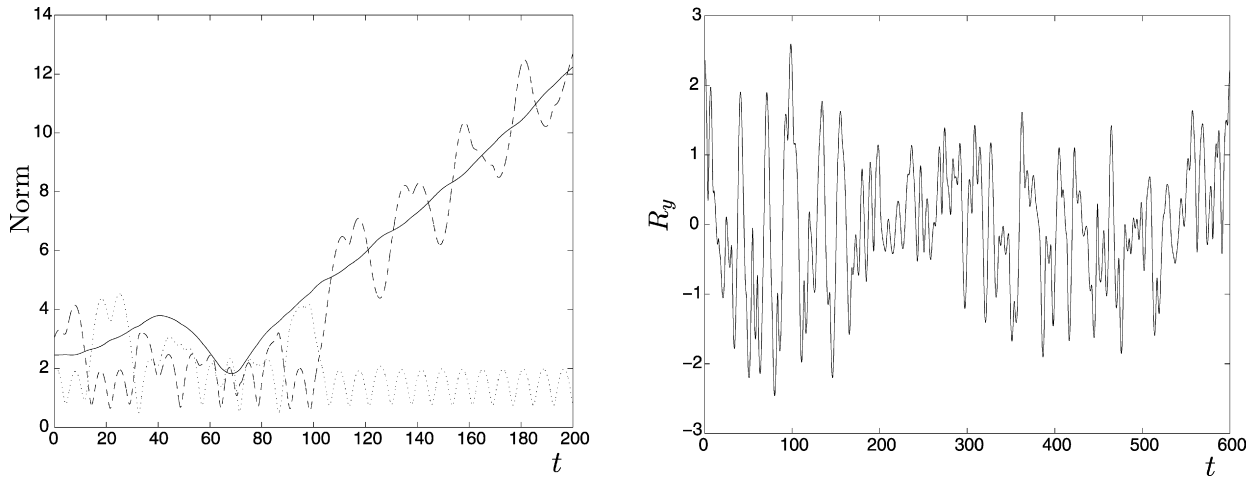

Fig. 16. Left figure: perturbation of the higher-energy (unstable) T-periodic solution of Fig. 9, with $\epsilon = 0.2$ and $\bar{\omega} = 0.4869$. We plot the B–B distance (continuous line), and the two distances A–B (dashed and dotted lines) as a function of time. The bounded component (dotted line) corresponds to $\|u_2 + u_1/2\|$ in this numerical run. Right figure: perturbation of the lower-energy (linearly stable) T-periodic solution of Fig. 9, with $\epsilon = 0.2$ and $\bar{\omega} = 0.4869$. We plot the vertical component of u_2 as a function of time. In both cases the initial perturbation of $\tilde{H}_\epsilon$ is lower that 5 percent.

Acknowledgements

This work has been supported by the French Ministry of Research through the CNRS Program ACI NIM (New Interfaces of Mathematics).

Appendix A. Normal periodic solutions near a triangular equilibrium

In this appendix we consider a T_0-periodic (nonconstant) solution $(R, \bar{\rho})$ of (21), (22) given by (24)–(26). We shall prove that Hypotheses 2, 3 are satisfied (for $r_2^0(t) = (0, R(T_0 t))^t$ and $\bar{u}_0 = (2\bar{\rho}, 0)^t$) when ρ^* is not a multiple of R^*, the hardness coefficient $h(\rho^*)$ defined by (27) does not vanish and $\alpha \approx 0$ (i.e. for a solution sufficiently close to the

triangular equilibrium (R^*, ρ^*)). For this purpose we study the explicit case $\alpha = 0$ and then treat the case $\alpha \approx 0$ by perturbation.

Firstly we check Hypothesis 2. Consider the fundamental solution matrix $M(t) \in \mathbb{R}^4$ ($M(0) = I$) of the linearized equation

$$\delta\ddot{r}_2 + T_0^2 D_{r_2}^2 V\big(\bar{u}_0, r_2^0\big)\delta r_2 = 0, \tag{67}$$

or equivalently $\frac{d\delta x}{dt} = \delta y$, $\frac{d\delta y}{dt} = -T_0^2 D_{r_2}^2 V(\bar{u}_0, r_2^0)\delta x$ (we have set $\delta x = \delta r_2$ for notational simplicity). The matrix $M(1)$ is called the *monodromy matrix* of (67). Then $\delta x \in \operatorname{Ker}\mathcal{L}$ if and only if δx is solution of (67) and $(\delta x, \delta y)(1) = (\delta x, \delta y)(0)$, or equivalently $(\delta x, \delta y)^t(0) \in \operatorname{Ker}(M(1) - I)$. Now let us determine the kernel of $M(1) - I$.

Firstly we examine the case $\alpha = 0$ of (24)–(26), where $\bar{u}_0 = (2\rho^*, 0)^t$, $r_2^0 = (0, R^*)^t$ and $T_0 = 2\pi/\omega_1^*$. The monodromy matrix has a double semi-simple eigenvalue $+1$ and a pair of complex conjugate eigenvalues $e^{\pm i 2\pi\omega_2^*/\omega_1^*}$ (see Section 3.1 for the expressions of ω_1^*, ω_2^*). If $\omega_2^*/\omega_1^* \notin \mathbb{N}$ (which is equivalent to assuming $\rho^*/R^* \notin \mathbb{N}$) then the eigenvalue $+1$ is exactly double.

Secondly, for $\alpha \neq 0$ small enough, $M(1)$ possesses an eigenvalue $+1$ which is at least double and nonsemi-simple because $h(\rho^*)$ does not vanish. Indeed this condition implies, for *small amplitude* periodic solutions of (21) oscillating around $R_0(\bar{\rho})$ and $\bar{\rho} \approx \rho^*$, that the derivative of frequency with respect to amplitude does not vanish (see [2], Section 26.7, p. 241). This property implies that the eigenvalue $+1$ of the associated monodromy matrix is nonsemi-simple (see [37] p. 693).

Using the above result for $\alpha = 0$ in conjunction with classical perturbation theory [11], we deduce that the eigenvalue $+1$ is exactly double for $\alpha \approx 0$. Since the eigenvalue $+1$ is nonsemi-simple for $\alpha \neq 0$, we thus have $\operatorname{Ker}(M(1) - I) = \langle(\dot{r}_2^0, \ddot{r}_2^0)^t(0)\rangle$ and $\operatorname{Ker}\mathcal{L} = \langle\dot{r}_2^0\rangle$. As a consequence Hypothesis 2 is satisfied for $\alpha \approx 0$ and $\alpha \neq 0$.

Lastly, in the case when $\alpha \to 0$ in (24)–(26) one obtains after lengthy but straightforward computations $h_2^0 \to -\frac{\rho^{*2}}{R^{*2}}(0, R^*)^t$ (we asymptotically solve Eq. (58)) and $\Delta_1 \to D^{*2}U''(D^*) > 0$ (this coefficient is defined by (62)).

References

[1] R. Abraham, J.E. Marsden, Foundations of Mechanics, second ed., Addison-Wesley Publishing Company, 1987.
[2] V.I. Arnol'd, Ordinary Differential Equations, Springer-Verlag, 1992.
[3] S. Aubry, Discrete breathers in anharmonic models with acoustic phonons, Ann. Inst. H. Poincaré Phys. Théor. 68 (1998) 381–420.
[4] B. Buffoni, J. Toland, Analytic Theory of Global Bifurcation, Princeton Ser. Appl. Math., 2003.
[5] T. Cretegny, R. Livi, M. Spicci, Breather dynamics in diatomic FPU chains, Physica D 119 (1998) 88–98.
[6] A. Dhooge, W. Govaerts, Yu.A. Kuznetsov, MATCONT: A Matlab package for numerical bifurcation analysis of ODEs, ACM Trans. Math. Software 29 (2) (2003) 141–164. Software cl_matcont available at: http://www.matcont.ugent.be/.
[7] E.J. Doedel, et al., Computation of periodic solutions of conservative systems with application to the 3-body problem, Int. J. Bifurcation and Chaos 13 (6) (2003) 1353–1381.
[8] J. Fura, S. Rybicki, Periodic solutions of second order Hamiltonian systems bifurcating from infinity, Ann. Institut H. Poincaré Anal. Non Linéaire 24 (3) (2007) 471–490.
[9] G. Iooss, D.D. Joseph, Elementary Stability and Bifurcation Theory, Springer, 1980.
[10] G. James, P. Noble, Weak coupling limit and localized oscillations in Euclidean invariant Hamiltonian systems, J. Nonlinear Sci. 18 (2008) 433–461.
[11] T. Kato, Perturbation Theory for Linear Operators, Springer-Verlag, 1966.
[12] H. Kielhöfer, Bifurcation Theory. An Introduction with Applications to PDEs, Applied Mathematical Sciences, vol. 156, Springer-Verlag, 2004.
[13] I.N. Kozin, I.M. Pavlichenkov, Bifurcation in rotational spectra of nonlinear AB_2 molecules, J. Chem. Phys. 104 (11) (1996) 4105–4113.
[14] I.N. Kozin, R.M. Roberts, J. Tennyson, Symmetry and structure of rotating H_3^+, J. Chem. Phys. 111 (1) (1999) 140–150.
[15] E. Lerman, T. Tokieda, On relative normal modes, C. R. Acad. Sci. Paris, Sér. I 328 (1999) 413–418.
[16] R.G. Littlejohn, K.A. Mitchell, V. Aquilanti, S. Cavalli, Body frames and frame singularities for three-atom systems, Phys. Rev. A 58 (5) (1998) 3705–3717.
[17] R. Livi, M. Spicci, R.S. MacKay, Breathers on a diatomic FPU chain, Nonlinearity 10 (1997) 1421–1434.
[18] R.S. MacKay, S. Aubry, Proof of existence of breathers for time-reversible or Hamiltonian networks of weakly coupled oscillators, Nonlinearity 7 (1994) 1623–1643.
[19] R.S. MacKay, Optic discrete breathers in Euclidean invariant systems, I. J. Nonlin. Sci. Num. Sim. 1 (2000) 99–103.
[20] J.L. Marin, S. Aubry, Breathers in nonlinear lattices: numerical calculation from the anticontinuous limit, Nonlinearity 9 (1996) 1501–1528.
[21] J.E. Marsden, T. Hughes, Mathematical Foundations of Elasticity, Dover Publications, 1994.
[22] J. Mawhin, M. Willem, Critical Point Theory and Hamiltonian Systems, Springer, New York, 1989.
[23] K.R. Meyer, Periodic Solutions of the N-body Problem, Lecture Notes in Mathematics, vol. 1719, Springer-Verlag, 1999.

[24] J. Montaldi, Persistance d'orbites périodiques relatives dans les systèmes hamiltoniens symétriques, C. R. Acad. Sci. Paris, Sér. I 324 (1997) 553–558.
[25] J.A. Montaldi, R.M. Roberts, Relative equilibria of molecules, J. Nonlinear Sci. 9 (1999) 53–88.
[26] J. Moser, Periodic orbits near an equilibrium and a theorem by Alan Weinstein, Comm. Pure Appl. Math. 29 (1976) 727–747.
[27] F.J. Muñoz-Almaraz, et al., Continuation of periodic orbits in conservative and Hamiltonian systems, Physica D 181 (2003) 1–38.
[28] J.-P. Ortega, Relative normal modes for nonlinear Hamiltonian systems, Proc. Roy. Soc. Edinburgh Sect. A 133 (2003) 665–704.
[29] J.-P. Ortega, T.S. Ratiu, Persistance et différentiabilité de l'ensemble des éléments critiques relatifs dans les systèmes hamiltoniens symétriques, C. R. Acad. Sci. Paris, Sér. I 325 (1997) 1107–1111.
[30] R. Prosmiti, S.C. Farantos, Periodic orbits, bifurcation diagrams and the spectroscopy of C_2H_2 system, J. Chem. Phys. 103 (9) (1995) 3299–3314.
[31] R. Prosmiti, S.C. Farantos, H. Guo, Assigning the transition from normal to local vibrational mode in SO_2 by periodic orbits, Chem. Phys. Lett. 311 (1999) 241–247.
[32] R. Prosmiti, et al., A combined classical/quantum study of the photodissociation dynamics of $NeBr_2$(B) near the Br_2(B) dissociation limit, Chem. Phys. Lett. 359 (2002) 229–236.
[33] R.M. Roberts, M.E.R. Sousa Dias, Bifurcation of relative equilibria, Nonlinearity 10 (1997) 1719–1738.
[34] L. Sbano, Symmetric solutions in molecular potentials, in: G. Gaeta, B. Prinari, S. Rauch, S. Terracini (Eds.), Symmetry And Perturbation Theory SPT2004, Proceedings of Cala Gonone workshop, Italy, 30 May–6 June 2004, World Scientific, 2005.
[35] L. Sbano, J. Southall, Periodic solutions of the N-body problem with Lennard–Jones potential, Mathematics Institute preprint, Univ. Warwick, 2007.
[36] D.S. Schmidt, Hopf's bifurcation theorem and the center theorem of Liapunov, in: J.E. Marsden, M. McCracken (Eds.), The Hopf Bifurcation Theorem and its Applications, in: Appl. Math. Sci., vol. 19, Springer, New York, 1976, pp. 95–104.
[37] J.-A. Sepulchre, R.S. MacKay, Localized oscillations in conservative or dissipative networks of weakly coupled autonomous oscillators, Nonlinearity 10 (1997) 679–713.
[38] A. Weinstein, Normal modes for nonlinear Hamiltonian systems, Invent. Math. 20 (1973) 47–57.
[39] C. Wulff, Persistence of relative equilibria in Hamiltonian systems with noncompact symmetry, Nonlinearity 16 (2003) 67–91.
[40] C. Wulff, Persistence of Hamiltonian relative periodic orbits, J. Geom. Phys. 48 (2003) 309–338.
[41] T. Yanao, K. Takatsuka, Kinematic effects associated with molecular frames in structural isomerization dynamics of clusters, J. Chem. Phys. 120 (2004) 8924–8936.
[42] T. Yanao, W.S. Koon, J.E. Marsden, I.G. Kevrekidis, Gyration-radius dynamics in structural transitions of atomic clusters, J. Chem. Phys. 126 (2007) 124102.
[43] A.A. Zevin, Global continuation of Lyapunov centre orbits in Hamiltonian systems, Nonlinearity 12 (1999) 1339–1349.